



HAL
open science

Copper at ancient Kerma: A diachronic investigation of alloys and raw materials

Frederik Rademakers, Georges Verly, Patrick Degryse, Frank Vanhaecke, Séverine Marchi, Charles Bonnet

► To cite this version:

Frederik Rademakers, Georges Verly, Patrick Degryse, Frank Vanhaecke, Séverine Marchi, et al.. Copper at ancient Kerma: A diachronic investigation of alloys and raw materials. *Advances in Archaeomaterials*, 2022, 3 (1), pp.1-18. 10.1016/j.aia.2022.01.001 . halshs-03696298

HAL Id: halshs-03696298

<https://shs.hal.science/halshs-03696298>

Submitted on 24 Dec 2023

HAL is a multi-disciplinary open access archive for the deposit and dissemination of scientific research documents, whether they are published or not. The documents may come from teaching and research institutions in France or abroad, or from public or private research centers.

L'archive ouverte pluridisciplinaire **HAL**, est destinée au dépôt et à la diffusion de documents scientifiques de niveau recherche, publiés ou non, émanant des établissements d'enseignement et de recherche français ou étrangers, des laboratoires publics ou privés.



Distributed under a Creative Commons Attribution - NonCommercial - NoDerivatives 4.0 International License



Copper at ancient Kerma: A diachronic investigation of alloys and raw materials



Frederik W. Rademakers^{a,b,*}, Georges Verly^c, Patrick Degryse^{b,d}, Frank Vanhaecke^e, Séverine Marchi^{f,g}, Charles Bonnet^{f,h}

^a Department of Scientific Research, British Museum, London, United Kingdom

^b Department of Earth and Environmental Sciences, KU Leuven, Leuven, Belgium

^c Royal Museums of Art and History, Brussels, Belgium

^d Faculty of Archaeology, Leiden University, Leiden, the Netherlands

^e Department of Analytical Chemistry, Ghent University, Ghent, Belgium

^f Mission suisse-franco-soudanaise de Kerma-Doukki Gel

^g CNRS, UMR 8167 (Orient & Méditerranée), équipe Mondes Pharaoniques, Paris, France

^h Académie des Inscriptions et Belles-Lettres, Paris, France

ARTICLE INFO

Keywords:

Nubian archaeology

Kerma

Archaeometallurgy

Provenance

Copper alloys

ABSTRACT

This paper describes the first comprehensive study of metal artefacts found at ancient Kerma, Sudan. Covering a period of several millennia, it investigates the development of copper alloy recipes as well as metal provenance through the trace element and lead isotope ratio analysis of forty-eight sampled objects. These include grave goods as well as production waste related to large-scale bronze casting performed at Kerma. This study is part of a wider evaluation of copper alloy production at Kerma through targeted workshop excavation, materials analysis, and experimental archaeology. The analytical results illustrate the gradual and flexible transition from arsenical copper to tin bronze alloys over time, in a pattern similarly observed in ancient Egypt. Trace element distributions and lead isotope ratios for copper used at Kerma are comparable to those of contemporary Egyptian artefacts too. These findings indicate the exploitation of ores similar to those mined at the Sinai Peninsula, although copper ore deposits in Nubia remain poorly characterized and thus difficult to identify as source candidates. Nonetheless, it can be suggested that metal provisioning networks along the Nile Valley likely overlapped to varying degrees over time. These results provide an important contribution to the mapping of technological exchanges that took place between ancient Egypt and Nubia.

1. Introduction

The history of the independent Nubian kingdom of Kerma covers almost a millennium,¹ from about 2500 BCE to 1500 BCE. The territory governed by the capital at Kerma (Bonnet, 2014, 2019) developed along the Nile Valley, between the first and the fifth cataracts (Fig. 1). This privileged geographical position enabled control of the supply of raw and precious materials heading primarily towards Kerma's powerful northern neighbour. The economy of Kerma—located at the crossroads between Egypt, Central Africa, and sub-Saharan regions such as present-day Kordofan, Darfur, and eastern Sudan—was based on an elaborate trading system but equally on the exploitation of surrounding alluvial lands, providing favourable conditions for the development of livestock and agriculture.

In this context, several craft productions were locally developed. They included pottery, faience, and metalwork. The latter is particularly well-known from the impressive metal objects found in the tombs of the Eastern Necropolis (Reisner, 1923: 176–206, Plate 48–50), from daily-life artefacts discovered in the capital (Marchi et al., in preparation), and from the recently reassessed bronze casting furnace near the *deffufa*, the main temple of the city (Bonnet, 2004: 33–38). This study offers an opportunity to gain a new perspective on copper metallurgy at Kerma, based on previously unpublished objects and fragments preserved in the warehouses of the Kerma-Doukki Gel archaeological mission.

Metal finds discussed in this paper date mainly to the Middle Kerma, Classic Kerma, and Meroitic periods, with one or two possible Napatan-period finds. (See Table 1 for Kerma's chronology.) The majority of finds

* Corresponding author at: Department of Scientific Research, British Museum, London, United Kingdom.

E-mail address: frademakers@britishmuseum.org (F.W. Rademakers).

¹ Nubia is geographically defined as the region between the first and sixth cataracts of the Nile, but the name can equally refer to cultural or ethnic groups inhabiting the wider Middle Nile region (e.g., Bonnet, 2019; Edwards, 2004; Török, 2009).



Fig. 1. Regional map showing the location of Kerma and other sites mentioned in the text.

can be dated to one of these periods, while in some cases contextual evidence allows only a general “Kerma period” identification. All finds derive from the city of Kerma and its Eastern and Western Necropolises (Bonnet et al., 2021: 171–73), with the exception of one find from Beit el-Sheitan (Bonnet, 2014: 209–14). New Kingdom copper alloys are not included here, as settlement discontinued at Kerma in favour of Doukki Gel following Egyptian conquest.

The analysed artefacts are relatively small finished objects such as rings, bracelets, chisels and rivets,² but they also include an ingot (intermediate product) and production waste (fragments and prills) from various contexts (Fig. 2, Table 2). Importantly, five spills associated with

² Most large metal objects, such as mirrors and daggers, are now in museum collections—in Khartoum, Kerma, Boston, and Geneva, for example. Therefore this study is biased towards smaller artefact types.

a Middle Kerma bronze casting furnace (Bonnet, 1986) have been analysed. Re-excavation and analysis of this furnace by the authors in 2018–2019 revealed that it was used for the casting of large (about 2 m²) bronze plates, testament to the extraordinary metallurgical skill present in the region at that time (Rademakers et al., 2019; for full results, see Verly et al., in preparation).

This study aims to provide, for the first time, an overview of the copper alloys in use at Kerma. Furthermore, the provenance of copper is investigated through the combined study of elemental compositions and lead isotope (LI) ratios. Recent work by the authors has strongly expanded the database on early Egyptian copper composition farther downstream in the Nile Valley, including trace element and LI ratio data (Rademakers et al., 2017, 2018a, 2018b, 2021a, 2021b; see also Abdel-Motelib et al., 2012; Anfinset, 2010; Hassan et al., 2015; Kmošek et al., 2018; Odler and Kmošek, 2020; Odler et al., 2021;

Table 1
Chronology of Kerma-Doukki Gel.

Period	Dates	Key features	Corresponding chronology Egypt
Pre-Kerma	3500 – 2500 BCE	Several settlements, including a proto-urban agglomeration on the site of the eastern necropolis.	Protodynastic Period to early Old Kingdom
Early Kerma	2500 – 2050 BCE	Foundation of the city. Development of the religious quarter and the eastern necropolis.	Old Kingdom and First Intermediate Period
Middle Kerma	2050 – 1750 BCE	Erection of fortified walls. Palaces and princely tombs.	Middle Kingdom
Classic Kerma	1750 – 1500 BCE	Expansion of the city and the defence system. Temples (<i>deffufa</i>) and royal tombs.	End of Middle Kingdom, Second Intermediate Period, start New Kingdom
Egyptian Occupation	1500 – 1080 BCE	Conquest of Nubia by Egyptian pharaohs of the New Kingdom. Destruction of the city of Kerma and foundation of a <i>menenu</i> at Doukki Gel.	New Kingdom
<i>End of Egyptian rule</i>	1080 – 800 BCE	Withdrawal of Egyptian authority. Period poorly documented.	Third Intermediate Period
Nubian Pharaohs	800 – 656 BCE	First Napatan kings and Twenty-fifth Dynasty pharaohs rule over a territory encompassing Egypt and Sudan.	Third Intermediate Period
Napatan	656 – 270 BCE	Kings from Napata. Restorations and constructions at Doukki Gel and Tabo.	Late Period
Meroitic	270 BCE – CE 340	Expansion of the western cemetery at Kerma. Political centre moved to Meroe. Continuation of constructions at Tabo and Doukki Gel. Occupation of the western cemetery at Kerma.	End of Late Period, Macedonian, Ptolemaic and Roman Periods

Pfeiffer, 2013; Rehren and Pernicka, 2014; Stos-Gale et al., 1995). Trace element and LI data were recently published for two Classic Kerma daggers by Rademakers et al. (2021b) and for one Classic Kerma artefact by Odler and Kmošek (2020). LI ratios for two Middle Kerma daggers reported by Young (1996) are insufficiently precise for provenance analysis (cf. Rademakers et al., 2021b),³ and elemental analysis of Kerma artefacts is otherwise limited (yet see Dunham, 1943;⁴ Vercoutter et al., 1960). Masson-Berghoff et al. (2018) provide further LI data and discussion for the Late Period (roughly coinciding with the Napatan and Meroitic periods at Kerma), expanding on limited earlier analyses for that period (e.g., Fleming, 1982).

These earlier studies provide essential comparatives to the dataset presented here. Indeed, one of the main issues to investigate is whether copper alloy compositions at Kerma evolved similarly to those in Egypt and to what degree copper provisioning systems were comparable and perhaps interrelated over time. Despite important contacts between Egypt and Nubia, Kerma remained independent for most of its history and was conquered only during the New Kingdom. While the Nubians had direct access to copper (and gold)⁵ deposits in the eastern desert (Klemm and Klemm, 2013) and possibly other major deposits to the west (in Darfur Province; Herbert, 1984; Master et al., 2016), important deposits in the Sinai were exploited only by the Egyptians and local (nomadic) populations. There are no indications for a Nubian (mining) presence on the Sinai Peninsula. However, Kerma's location at the intersection of trans-Saharan trade routes running east–west across the

continent and the Nile Valley, extending north into Egypt and south into East and Central Africa, provided it with access to a highly diverse trade network. Beyond interactions with Egypt, copper may very well have been amongst the commodities exchanged with different regions in Africa and on the Arabian Peninsula.

2. Materials and methods

All metal artefacts held at the Kerma excavation house were studied during the excavation season of December 2018, which included qualitative surface handheld X-ray fluorescence analysis to identify copper alloys and contaminants. Forty-eight artefacts were sampled, covering the periods for which metalwork is attested and the different metal alloys present in the assemblage. The samples and their contextual data are presented in Table 2. A selection of artefacts is illustrated in Fig. 3; a complete overview is provided in the online supplementary materials (OSM), including photographic documentation, artefact dimensions, and artefact weight.

Metal samples were either clipped using steel cutting pliers or drilled using a clean TiN-coated 1 mm steel drill bit to obtain core material. Prior to sampling, surface corrosion was mechanically removed from the sampling area of all artefacts with a Dremel rotary tool, steel brush, or drill bit. However, more than half of the artefacts contained minor to important intergranular corrosion and some were corroded throughout, as indicated in Table 2. Samples were exported with the permission of the National Corporation for Antiquities and Museums of the Republic of the Sudan for analysis at the KU Leuven in Belgium. Three samples (MAH 27796 E, F, and G) related to the bronze casting furnace were taken from casting spills held at the Musées d'art et d'histoire de Genève by the curator.⁶

All samples were completely dissolved following a high-temperature acid digestion procedure (except for the lead alloy COT90/3, which was

³ Note that Odler and Kmošek (2020: 138) do not interpret this data with the necessary caution.

⁴ Dunham presents the results of OES analysis of eleven Kerma artefacts and eight Middle Kingdom Egyptian artefacts. Only copper, tin, and lead concentrations are reported.

⁵ Gold artefacts (mainly sheet gold) are included among the Kerma-period metal assemblage but are not discussed here. Handheld XRF surface analysis shows that these mostly consist of fairly pure gold with low concentrations of silver and copper. Silver jewelry (with low gold, copper, and lead concentrations) is encountered as well.

⁶ Qualitative XRF analysis of copper alloy artefacts currently held at the Kerma Museum and the Musées d'art et d'histoire de Genève is being prepared for publication and is not further discussed here.

Table 2
Sample Overview.

Sample	Inv n°	Date	Artefact type	Corrosion	Excavation date	Site	Stratigraphic unit, coordinates
KF_104	F046	Middle Kerma Period	Prill	/	16/12/2018	Kerma, city	Casting furnace, US052, F8c
KF_100	F003	Middle Kerma Period	Prill	/	09–12–18	Kerma, city	Casting furnace, US048 (in contact with US002, 4C)
27796 E	MAH 027796 E	Middle Kerma Period	Casting spill	/	11–01–81	Kerma, city	Casting furnace, associated with crucible - F8 (?)
27796 F	MAH 027796 F	Middle Kerma Period	Casting spill	/	11–01–81	Kerma, city	Casting furnace, associated with crucible - F8 (?)
27796 G	MAH 027796 G	Middle Kerma Period	Casting spill	/	11–01–81	Kerma, city	Casting furnace, associated with crucible - F8 (?)
KF_4	KV736	Middle Kerma Period	Needle	Mostly corroded, minor metallic phase	27–12–90	Kerma, city	Deffufa - Western annexes - North of the religious building L
KF_28	KV660	Middle Kerma Period	Chisel	/	18–12–99	Kerma, city	N-W Quarter
KF_17	CE12	Middle Kerma Period	Disc	Corroded throughout	01–12–86	Eastern Necropolis	CE 12, Grave T121/3
KF_18	CET92/4	Middle Kerma Period	Rivet	/	11–01–84	Eastern Necropolis	CE 10, Grave T92
KF_19	CET111/2	Middle Kerma Period	Rivet	/	01–01–86	Eastern Necropolis	CE 10, Grave T111
KF_10	KV493	Middle Kerma Period (end of Middle Kerma Period)	Uraeus	/	07–12–93	Kerma, city	Secondary agglomeration - Sector 60 - Outside Chapel E VIII
KF_11	KV496A	Middle Kerma Period (end of Middle Kerma Period)	Rod	Inter-granular (cuprite) corrosion	19–12–93	Kerma, city	Secondary agglomeration - Sector 59, Building M133 - S212,00/W195,00
KF_12	KV496B	Middle Kerma Period (end of Middle Kerma Period)	Rod	Mostly corroded, minor metallic phase	19–12–93	Kerma, city	Secondary agglomeration - Sector 59, Building M133 - S212,00/W195,00
KF_13	KV496C	Middle Kerma Period (end of Middle Kerma Period)	Rod	Mostly corroded, minor metallic phase	19–12–93	Kerma, city	Secondary agglomeration - Sector 59, Building M133 - S212,00/W195,00
KF_6	KV036	End of Middle Kerma Period	Rod/needle	Corroded throughout	18–12–77	Kerma, city	Sector 1 - Building M1 - S73,00/W3,00
KF_24	KV742	End of Middle Kerma Period (possibly Classic Kerma Period)	Prill	Corroded throughout	19–12–82	Kerma, city	Sector 10 - Building M27 - S160,00/W105,00
KF_25	KV743	End of Middle Kerma Period (possibly Classic Kerma Period)	Ingot	/	19–12–82	Kerma, city	Sector 10 - Building M27 - S160,00/W105,00
KF_26	KV744	End of Middle Kerma Period (possibly Classic Kerma Period)	Rod	Corroded throughout	19–12–82	Kerma, city	Sector 10 - Building M27 - S160,00/W105,00
KF_27	KV745	End of Middle Kerma Period (possibly Classic Kerma Period)	Ring (?)	Corroded throughout	19–12–82	Kerma, city	Sector 10 - Building M27 - S160,00/W105,00
KF_32	BES003	End of Middle Kerma Period - Classic Kerma Period	Rivet	/	01–12–90	Beit el-Sheitan	Sector 63 - Building M320-M321
KF_16	KV422A	Classic Kerma Period (possibly Middle Kerma Period)	Ring (?)	Mostly corroded, minor metallic core	06–01–92	Kerma, city	Sector 51 - S10,00–20,00/W164,00
KF_29	KV422B	Classic Kerma Period (possibly Middle Kerma Period)	Prill	Corroded throughout	06–01–92	Kerma, city	Sector 51 - S10,00–20,00/W164,00
KF_30	KV422C	Classic Kerma Period (possibly Middle Kerma Period)	Prill	Corroded throughout	06–01–92	Kerma, city	Sector 51 - S10,00–20,00/W164,00
KF_31	KV422D	Classic Kerma Period (possibly Middle Kerma Period)	Fragment	Corroded throughout	06–01–92	Kerma, city	Sector 51 - S10,00–20,00/W164,00
KF_5	KV132	Classic Kerma Period	Rod	Mostly corroded, minor metallic phase	24–12–81	Kerma, city	Deffufa - Western annexes, Religious building L
KF_7	KV001	Classic Kerma Period	Rod	Corroded throughout	27–12–75	Kerma, city	Sector 48 - Eastern fortifications, filling in the southern well
KF_8	KV307	Classic Kerma Period	Plaque	Mostly corroded, minor metallic core	27–01–87	Kerma, city	Sector 48 - Eastern fortifications
KF_9	KV302	Classic Kerma Period	Needle	Mostly corroded, minor metallic core	26–11–87	Kerma, city	Sector 48 - Eastern fortifications
KF_15	KV507	Classic Kerma Period	Rod	Mostly metallic, minor inter-granular corrosion	03–01–94	Kerma, city	Secondary agglomeration - Sector 59, Northern fortifications - S190,00/W185,00

(continued on next page)

Table 2 (continued)

Sample	Inv n°	Date	Artefact type	Corrosion	Excavation date	Site	Stratigraphic unit, coordinates
KF_82	KV746	Kerma Period (no specification possible)	Needle	Corroded throughout	1984–1986	Kerma, city	Sector 52, "Grande hutte"
KF_22	KV747	Kerma Period (no specification possible)	Bracelet	/	05–01–95	Kerma, city	M304/Zeriba audience hall
KF_80	KV738	Kerma Period (no specification possible)	Hook fragment (?)	Corroded throughout	08–01–98	Kerma, city	Secondary agglomeration - S-W quarter, surface
KF_81	KV739	Kerma Period (no specification possible)	Needle	Corroded throughout	01–01–98	Kerma, city	Eastern area
KF_84	KV740	Kerma Period (no specification possible)	Fragment	/	01–01–98	Kerma, city	Eastern area
KF_39	COT90/3	Meroitic Period	Sieve	/	1988–89	Kerma, city / Western Necropolis	Grave T90
KF_20	CVT12/4	Meroitic Period	Fragment	Corroded throughout	27–12–80	Kerma, city / Western Necropolis	Grave T12
KF_21	CVT13	Meroitic Period	Plaque	Corroded throughout	27–12–80	Kerma, city / Western Necropolis	Grave T13
KF_33	COT79/6	Meroitic Period	Bent rod	/	1988–89	Kerma, city / Western Necropolis	Grave T79
KF_34	COT79/6	Meroitic Period	Folded rod	/	1988–89	Kerma, city / Western Necropolis	Grave T79
KF_35	COT79/6	Meroitic Period	Folded rod	/	1988–89	Kerma, city / Western Necropolis	Grave T79
KF_36	COT79/6	Meroitic Period	Ring	/	1988–89	Kerma, city / Western Necropolis	Grave T79
KF_37	COT79/6	Meroitic Period	Ring	/	1988–89	Kerma, city / Western Necropolis	Grave T79
KF_38	COT79/6	Meroitic Period	Ring	/	1988–89	Kerma, city / Western Necropolis	Grave T79
KF_1	KV122A	Meroitic Period	Ring	Minor inter-granular corrosion	21–12–80	Kerma, city / Western Necropolis	Grave
KF_2	KV122B	Meroitic Period	Ring	Mostly corroded, minor metallic core	21–12–80	Kerma, city / Western Necropolis	Grave
KF_3	KV122C	Meroitic Period	Ring	Corroded throughout	21–12–80	Kerma, city / Western Necropolis	Grave
KF_14	KV748	Meroitic or Napatean Period	Rod	Corroded throughout	22–12–93	Kerma, city / Western Necropolis	Secondary agglomeration - Sector 41 - S180,00/W200,00, near Grave T106
KF_23	COT114/1	Possibly Napatean Period	Bracelet	/	13–12–94	Kerma, city / Western Necropolis	Grave T114 (north of building M135)

directly dissolved in 1 M HNO₃). One aliquot was retained for elemental analysis by inductively coupled plasma optical emission spectroscopy (ICP-OES), while the remainder was used for lead isolation and lead isotope analysis by multi-collector inductively coupled plasma mass spectrometry (MC-ICP-MS). Full details of sample preparation and laboratory procedures are discussed by Rademakers et al. (2020).

Samples of the most strongly corroded artefacts are associated with increased levels of barium, chromium, iron, magnesium, manganese, and titanium, as well as frequently elevated phosphorus and sulphur (cf. OSM: Fig. 1). These elements, deriving from the burial environment, are incorporated into the artefacts' corrosion minerals and are thus not considered informative of ancient alloy compositions (even though iron, phosphorus, and sulphur may partially reflect ancient metal compositions). Analytical totals (ICP-OES) for the most strongly corroded artefacts are often around 60–70 wt% and even down to about 30 wt% (indicative of complete mineralisation). Element concentrations for such strongly corroded artefacts are considered indicative. These may be relatively enriched or depleted in particular corrosion products compared to the original metallic phase, with copper dissolution being the main corrosion phenomenon (Robbiola et al., 1998). Even if relative depletion may differ between elements, orders of magnitude can provide useful information on typical elements associated with copper alloys (Ag, As, Au, Bi, Co, Ni, Pb, Sb, and Sn; Zn tends to be strongly depleted), for which environmental contamination is expected to be minimal (Dussubieux et al., 2008; Mödinger and Piccardo, 2013; Moreau and Hancock, 1999).

Elemental data are presented in Table 3 as non-normalised concentrations (Cu in wt%; all other elements in µg/g). Lower totals are obtained for more strongly corroded artefacts: these concentration data should therefore be interpreted cautiously. Lead isotope ratios are presented in Table 4 and consistently plotted with their 95% confidence intervals.

3. Results

3.1. Copper alloys

The entire assemblage consists of copper alloys. Arsenic and tin are the main components, ranging from 0% to 1.2% and 0% to 10%, respectively, while lead concentrations are mostly below 0.5%.

Arsenic concentrations vary between 0.3% and 1.2% for the Middle Kerma artefacts and appear to decrease slightly for the Classic Kerma period (0.1%–1.2%, except for KV422D, with only 150 µg/g).⁷ By the Meroitic period, arsenic concentrations have decreased significantly: they are mostly below 0.1% and in two rings even below 100 µg/g.

Tin is present as an alloy component throughout the assemblage, except for the Classic Kerma artefacts. The Middle Kerma artefacts contain

⁷ All plots for Classic Kerma artefacts include daggers E.06118 and E.07391 (data from Rademakers et al., 2021b).

Table 3

Elemental Concentrations for Sampled Artefacts (all in µg/g, except for Cu in wt%).

MKP: Middle Kerma Period, CKP: Classic Kerma Period, KP: Kerma Period (no specification possible), MP: Meroitic Period, NP: Napatean Period

Sample	Inv n°	Dating	Artefact type	Cu (%)	Ag	As	Au	Ba	Bi	Co	Cr	Fe	Mg	Mn	Ni	P	Pb	S	Sb	Se	Sn	Te	Ti	Zn	Totals
KF_104	F046	MKP	Prill	72.3	110	5200	17	25	35	95	12	8800	710	20	220	220	2300	1100	45	20	25,000	120	290	45	76.8
KF_100	F003	MKP	Prill	81.7	170	7600	50	3	< 70	110	< 5	2200	< 60	< 3	480	< 80	4000	1100	90	50	76,000	110	< 5	45	90.9
27796 E	MAH 027796 E	MKP	Casting spill	89.2	120	6400	15	2	< 70	130	< 5	2500	< 60	2	560	< 80	6100	770	80	30	70,000	95	19	< 30	97.9
27796 F	MAH 027796 F	MKP	Casting spill	84.0	240	9300	30	7	70	160	< 5	8800	< 60	2	510	85	2000	510	130	< 10	53,000	85	20	< 30	91.5
27796 G	MAH 027796 G	MKP	Casting spill	89.4	220	11,000	40	5	75	170	< 5	2600	< 60	< 3	560	95	2100	580	125	30	40,000	120	< 1	35	95.2
KF_4	KV736	MKP	Needle	89.5	110	1100	< 10	13	< 70	230	7	2400	540	45	750	170	130	3300	90	< 10	580	65	250	130	90.5
KF_28	KV660	MKP	Chisel	91.9	520	9700	115	4	35	45	< 10	1200	< 20	8	360	15	1300	1400	180	45	15,000	130	7	50	94.9
KF_17	CE12	MKP	Disc	85.6	560	11,000	120	14	7	7	15	2000	430	40	260	90	60	1600	300	45	180	130	370	20	87.4
KF_18	CET92/4	MKP	Rivet	93.6	390	12,000	85	< 2	< 10	20	< 10	2200	< 20	< 5	300	15	360	340	290	55	16,000	150	< 5	30	96.9
KF_19	CET111/2	MKP	Rivet	94.4	320	7400	960	< 2	< 10	160	< 10	310	< 20	< 5	1700	13	300	810	150	40	530	150	< 5	30	95.7
KF_10	KV493	(End of) MKP	Uraeus	81.1	200	3400	35	< 2	25	25	< 10	1100	90	< 5	360	40	3200	1000	370	40	98,000	110	12	9	91.9
KF_11	KV496A	(End of) MKP	Rod	90.8	160	3800	18	< 2	< 10	340	< 10	1600	125	9	750	40	1000	520	50	< 15	8400	110	50	50	92.5
KF_12	KV496B	(End of) MKP	Rod	83.8	400	8900	35	< 2	40	15	< 10	520	240	35	290	180	1400	650	130	75	16,000	190	45	10	86.7
KF_13	KV496C	(End of) MKP	Rod	80.1	140	9000	15	4	115	360	< 5	8800	530	55	670	190	3100	3600	120	40	43,000	105	110	40	87.1
KF_6	KV036	End of MKP	Rod/needle	52.7	270	6800	16	95	< 70	8	25	4600	1100	40	40	260	570	340	105	17	16,000	< 50	700	< 30	55.8
KF_24	KV742	End of MKP (poss CKP)	Prill	44.7	660	5500	5400	65	< 70	95	30	6700	2400	150	240	3400	1300	2500	160	< 10	24,000	< 50	1300	120	50.1
KF_25	KV743	End of MKP (poss CKP)	Ingot	80.1	100	2000	60	75	< 70	40	16	4700	920	45	410	480	330	990	< 60	< 10	8700	75	460	90	82.0
KF_26	KV744	End of MKP (poss CKP)	Rod	32.6	75	2100	45	125	< 70	55	25	9100	2600	260	510	7000	320	20,000	< 60	< 10	49,000	< 50	1100	35	41.8
KF_27	KV745	End of MKP (poss CKP)	Ring (?)	43.5	55	2400	< 10	80	< 70	60	340	16,000	1800	110	210	8200	2600	16,000	< 60	< 10	18,000	< 50	930	45	50.2
KF_32	BES003	End of MKP - CKP	Rivet	89.9	220	1900	40	25	< 70	5	20	3400	850	45	280	240	35	270	85	220	210	190	520	180	90.7
KF_16	KV422A	CKP (poss MKP)	Ring (?)	74.0	6	7200	< 10	20	< 70	125	8	7600	720	30	940	220	310	5400	95	< 10	< 100	50	250	280	76.4
KF_29	KV422B	CKP (poss MKP)	Prill	73.0	90	3200	95	95	< 70	12	7	2000	490	45	115	14,000	180	4900	115	80	780	50	310	< 30	75.7
KF_30	KV422C	CKP (poss MKP)	Prill	71.6	40	2300	17	20	300	4	8	1900	710	40	9	12,000	710	24,000	540	350	< 100	480	290	< 30	76.0
KF_31	KV422D	CKP (poss MKP)	Fragment	7.5	12	150	12	170	70	90	20	176,000	970	60	105	1800	75	32,000	< 60	< 10	< 100	80	1600	95	28.9
KF_5	KV132	CKP	Rod	70.9	80	3300	< 10	35	< 70	145	13	4800	1500	75	780	670	930	1300	< 60	14	3200	60	770	65	72.7
KF_7	KV001	CKP	Rod	52.2	55	1200	70	40	< 70	14	17	3300	1000	35	115	770	110	5600	200	< 10	170	< 50	510	< 30	53.5
KF_8	KV307	CKP	Plaque	92.9	85	6900	18	6	< 70	110	7	3700	85	3	430	< 80	890	1700	130	25	210	85	35	110	94.4
KF_9	KV302	CKP	Needle	29.1	8	2500	13	115	< 70	10	25	10,000	2700	160	40	5700	1300	38,000	115	< 10	580	< 50	1200	35	35.3
KF_15	KV507	CKP	Rod	94.4	110	12,000	16	2	< 70	55	< 5	2000	125	7	330	< 80	900	3600	330	45	740	105	75	< 30	96.5
KF_82	KV746	KP	Needle	62.0	95	5400	9	35	< 70	11	18	4600	660	45	40	1200	23,000	15,000	135	30	57,000	70	560	< 30	72.8
KF_22	KV747	KP	Bracelet	88.7	230	1100	14	< 3	< 70	60	< 5	370	< 60	6	240	< 80	2500	500	250	< 10	89,000	85	6	< 30	98.1
KF_80	KV738	KP	Hook fragment (?)	76.3	480	2600	50	25	< 70	11	8	3200	790	25	100	1100	290	2600	210	30	410	75	420	40	77.5
KF_81	KV739	KP	Needle	68.7	280	960	40	50	< 70	70	14	4200	1100	85	330	4600	75	3900	< 60	80	< 100	100	620	< 30	70.3
KF_84	KV740	KP	Fragment	74.4	210	6600	40	35	< 70	50	16	4400	1100	65	400	3600	630	760	280	11	3700	70	630	60	76.7
KF_39	COT90/3	MP	Sieve	0.1	90	30	< 5	3	65	6	11	270	65	5	6	< 100	818,000	130	240	< 50	83,000	< 10	15	13	90.3
KF_20	CVT12/4	MP	Fragment	57.7	70	1100	15	30	< 30	35	18	4600	1400	55	35	310	2500	1700	100	< 50	57,000	75	590	25	64.6
KF_21	CVT13	MP	Plaque	62.4	220	800	25	30	< 30	4	12	3900	1200	50	130	920	6900	2200	120	< 50	48,000	90	630	12	68.9
KF_33	COT79/6	MP	Bent rod	87.1	240	140	6	< 3	75	2	< 3	1000	< 40	1	75	< 100	60	180	75	135	98,000	115	< 5	< 10	97.1
KF_34	COT79/6	MP	Folded rod	87.2	440	500	10	10	95	10	3	2300	75	20	90	1300	90	830	710	60	1000	115	25	8	88.0
KF_35	COT79/6	MP	Folded rod	84.7	460	480	10	11	120	9	3	2200	80	4	85	660	85	1300	690	50	760	105	25	< 10	85.4
KF_36	COT79/6	MP	Ring	95.4	450	430	6	12	< 30	12	9	4000	380	19	100	600	105	2000	550	60	2400	145	180	35	96.6
KF_37	COT79/6	MP	Ring	84.1	500	180	11	< 3	55	5	< 3	3200	35	2	130	< 100	550	260	180	40	71,000	110	13	< 10	91.8
KF_38	COT79/6	MP	Ring	84.6	500	230	13	2	< 30	5	3	3700	55	2	135	< 100	550	320	220	55	89,000	110	14	< 10	94.1
KF_1	KV122A	MP	Ring	84.4	330	1300	40	2	85	50	< 3	3000	45	6	460	< 100	14,000	980	240	< 50	78,000	125	20	11	94.2
KF_2	KV122B	MP	Ring	77.0	550	30	40	9	< 30	3	4	1600	220	15	95	270	520	520	70	25	68,000	90	150	< 10	84.2
KF_3	KV122C	MP	Ring	69.6	390	15	35	9	< 30	2	4	1000	160	25	45	1400	4400	1700	30	< 50	47,000	80	70	9	75.2
KF_14	KV748	MP/NP	Rod	46.3	35	280	45	95	< 30	260	30	12,000	5200	470	550	590	50	730	13	< 50	4800	35	2000	95	48.6
KF_23	COT114/1	Poss. NP	Bracelet	84.2	145	760	25	4	70	320	3	1500	310	10	350	220	9000	760	200	< 50	69,000	100	110	65	92.5

Table 4

Pb Isotope Ratios for Sampled Artefacts.

MKP: Middle Kerma Period, **CKP:** Classic Kerma Period, **KP:** Kerma Period (no specification possible), **MP:** Merotic Period, **NP:** Napatean Period

Sample	Inv n°	Dating	Artefact type	$^{206}\text{Pb}/^{204}\text{Pb}$	$^{207}\text{Pb}/^{204}\text{Pb}$	$^{208}\text{Pb}/^{204}\text{Pb}$	$^{207}\text{Pb}/^{206}\text{Pb}$	$^{208}\text{Pb}/^{206}\text{Pb}$	σ $^{206}\text{Pb}/^{204}\text{Pb}$	σ $^{207}\text{Pb}/^{204}\text{Pb}$	σ $^{208}\text{Pb}/^{204}\text{Pb}$	σ $^{207}\text{Pb}/^{206}\text{Pb}$	σ $^{208}\text{Pb}/^{206}\text{Pb}$
KF_104	F046	MKP	Prill	18.468	15.665	38.550	0.84818	2.08734	0.005	0.003	0.009	0.00007	0.00014
KF_100	F003	MKP	Prill	18.650	15.704	38.837	0.84206	2.08245	0.003	0.002	0.006	0.00004	0.00011
27796 E	MAH 27796 E	MKP	Casting spill	18.635	15.697	38.796	0.84238	2.08193	0.003	0.002	0.006	0.00003	0.00008
27796 F	MAH 27796 F	MKP	Casting spill	18.561	15.678	38.682	0.84469	2.08405	0.008	0.006	0.017	0.00009	0.00016
27796 G	MAH 27796 G	MKP	Casting spill	18.569	15.688	38.702	0.84483	2.08421	0.002	0.002	0.005	0.00003	0.00010
KF_4	KV736	MKP	Needle	18.298	15.675	38.415	0.85662	2.09929	0.003	0.003	0.008	0.00004	0.00011
KF_28	KV660	MKP	Chisel	18.775	15.707	38.958	0.83652	2.07489	0.004	0.004	0.008	0.00004	0.00011
KF_17	CE12	MKP	Disc	18.778	15.679	38.786	0.83496	2.06544	0.004	0.003	0.007	0.00005	0.00012
KF_18	CET92/4	MKP	Rivet	18.584	15.677	38.682	0.84360	2.08151	0.004	0.004	0.009	0.00005	0.00012
KF_19	CET111/2	MKP	Rivet	18.566	15.646	38.559	0.84268	2.07684	0.003	0.003	0.008	0.00006	0.00012
KF_10	KV493	(End of) MKP	Uraeus	18.465	15.679	38.588	0.84915	2.08976	0.005	0.004	0.010	0.00004	0.00011
KF_11	KV496A	(End of) MKP	Rod	18.526	15.672	38.624	0.84597	2.08490	0.004	0.004	0.009	0.00007	0.00016
KF_12	KV496B	(End of) MKP	Rod	18.606	15.689	38.739	0.84322	2.08206	0.004	0.003	0.009	0.00005	0.00012
KF_13	KV496C	(End of) MKP	Rod	18.518	15.678	38.602	0.84665	2.08454	0.004	0.003	0.010	0.00005	0.00014
KF_6	KV036	End of MKP	Rod/needle	18.505	15.662	38.633	0.84636	2.08768	0.003	0.003	0.007	0.00005	0.00010
KF_24	KV742	End of MKP (poss CKP)	Prill	18.649	15.679	38.765	0.84080	2.07870	0.004	0.003	0.009	0.00006	0.00011
KF_25	KV743	End of MKP (poss CKP)	Ingot	18.787	15.692	38.778	0.83527	2.06414	0.003	0.003	0.006	0.00006	0.00010
KF_26	KV744	End of MKP (poss CKP)	Rod	18.620	15.648	38.664	0.84035	2.07645	0.004	0.003	0.009	0.00004	0.00013
KF_27	KV745	End of MKP (poss CKP)	Ring (?)	18.794	15.694	38.895	0.83508	2.06958	0.007	0.006	0.015	0.00008	0.00018
KF_32	BES003	End of MKP - CKP	Rivet	18.509	15.670	38.577	0.84661	2.08428	0.003	0.003	0.006	0.00006	0.00011
KF_16	KV422A	CKP (poss MKP)	Ring (?)	18.925	15.702	38.982	0.82969	2.05982	0.003	0.003	0.008	0.00005	0.00012
KF_29	KV422B	CKP (poss MKP)	Prill	18.418	15.664	38.520	0.85046	2.09138	0.004	0.004	0.009	0.00005	0.00012
KF_30	KV422C	CKP (poss MKP)	Prill	19.098	15.723	39.376	0.82333	2.06182	0.007	0.006	0.015	0.00007	0.00014
KF_31	KV422D	CKP (poss MKP)	Fragment	18.726	15.668	38.678	0.83672	2.06551	0.004	0.003	0.009	0.00005	0.00009
KF_5	KV132	CKP	Rod	18.637	15.666	38.743	0.84059	2.07881	0.004	0.003	0.009	0.00003	0.00013
KF_7	KV001	CKP	Rod	18.624	15.690	38.860	0.84247	2.08659	0.004	0.003	0.008	0.00005	0.00009
KF_8	KV307	CKP	Plaque	18.100	15.578	37.905	0.86066	2.09423	0.004	0.003	0.008	0.00005	0.00010
KF_9	KV302	CKP	Needle	18.852	15.681	39.000	0.83180	2.06878	0.004	0.004	0.009	0.00005	0.00012
KF_15	KV507	CKP	Rod	18.803	15.668	38.963	0.83326	2.07212	0.004	0.003	0.009	0.00005	0.00011
KF_82	KV746	KP	Needle	18.419	15.658	38.592	0.85012	2.09524	0.003	0.003	0.007	0.00003	0.00010
KF_22	KV747	KP	Bracelet	18.506	15.680	38.691	0.84731	2.09071	0.003	0.003	0.006	0.00004	0.00011
KF_80	KV738	KP	Hook fragment (?)	18.774	15.674	38.913	0.83488	2.07266	0.003	0.003	0.008	0.00004	0.00012
KF_81	KV739	KP	Needle	18.671	15.637	38.740	0.83751	2.07482	0.004	0.003	0.008	0.00004	0.00012
KF_84	KV740	KP	Fragment	18.660	15.669	38.723	0.83975	2.07527	0.009	0.007	0.018	0.00008	0.00019
KF_39	COT90/3	MP	Sieve	18.737	15.687	38.982	0.83720	2.08050	0.003	0.002	0.006	0.00005	0.00009
KF_20	CVT12/4	MP	Fragment	18.538	15.662	38.695	0.84484	2.08732	0.003	0.002	0.006	0.00004	0.00009
KF_21	CVT13	MP	Plaque	18.822	15.696	38.900	0.83382	2.06661	0.004	0.003	0.008	0.00004	0.00011
KF_33	COT79/6	MP	Bent rod	18.407	15.661	38.466	0.85083	2.08977	0.002	0.002	0.005	0.00004	0.00009
KF_34	COT79/6	MP	Folded rod	18.247	15.653	38.338	0.85788	2.10110	0.003	0.002	0.006	0.00003	0.00008
KF_35	COT79/6	MP	Folded rod	18.267	15.657	38.357	0.85710	2.09979	0.002	0.002	0.005	0.00004	0.00011
KF_36	COT79/6	MP	Ring	18.334	15.661	38.428	0.85420	2.09605	0.002	0.002	0.004	0.00003	0.00009
KF_37	COT79/6	MP	Ring	18.277	15.652	38.383	0.85637	2.10006	0.003	0.002	0.006	0.00004	0.00008
KF_38	COT79/6	MP	Ring	18.285	15.653	38.393	0.85606	2.09973	0.003	0.002	0.006	0.00003	0.00009
KF_1	KV122A	MP	Ring	18.825	15.697	38.904	0.83378	2.06650	0.003	0.002	0.005	0.00005	0.00008
KF_2	KV122B	MP	Ring	18.474	15.657	38.597	0.84752	2.08928	0.003	0.002	0.006	0.00004	0.00008
KF_3	KV122C	MP	Ring	18.444	15.653	38.580	0.84864	2.09169	0.003	0.002	0.007	0.00004	0.00009
KF_14	KV748	MP/NP	Rod	18.354	15.671	38.496	0.85380	2.09741	0.002	0.002	0.005	0.00004	0.00007
KF_23	COT114/1	Poss. NP	Bracelet	18.580	15.675	38.674	0.84368	2.08150	0.004	0.003	0.008	0.00004	0.00010

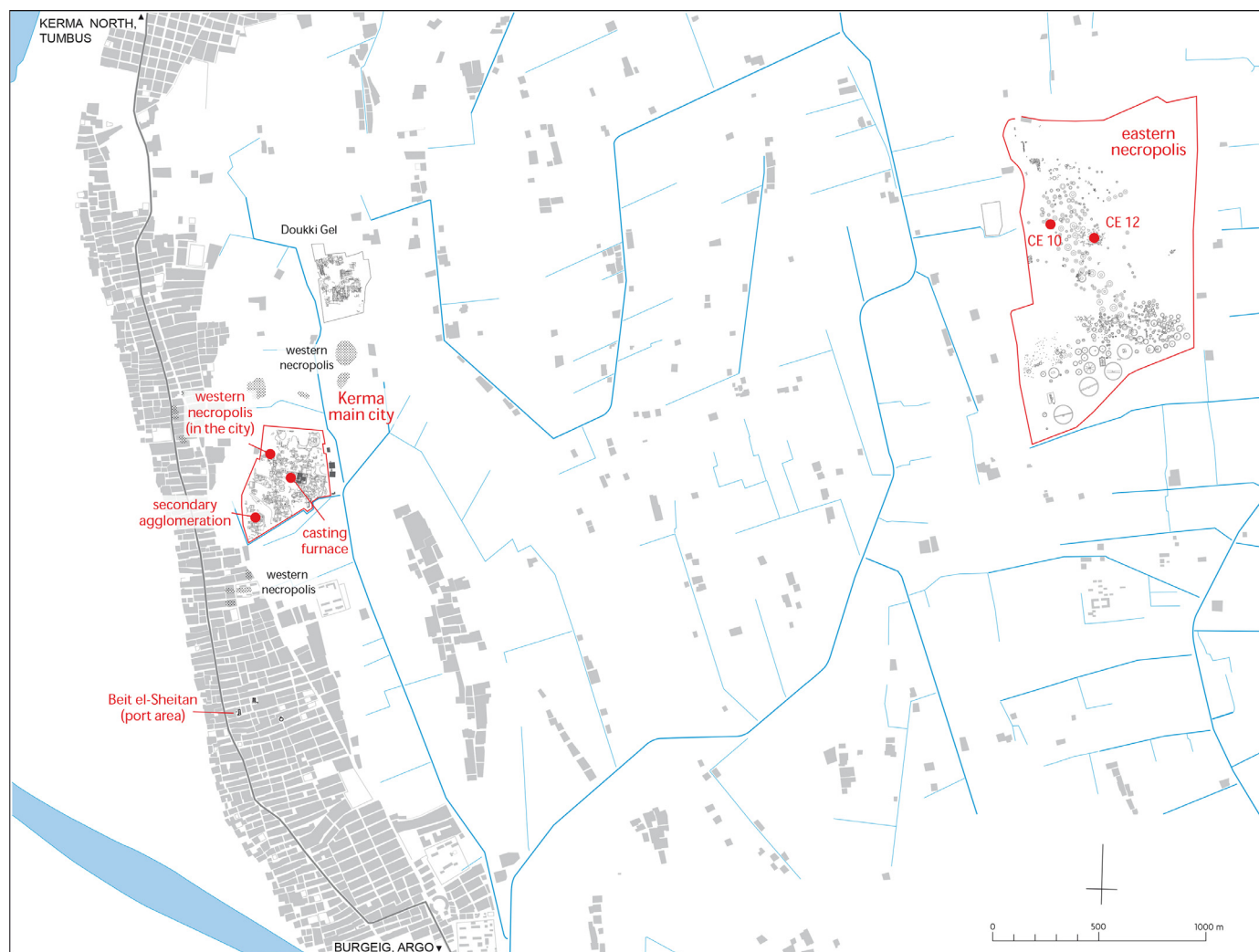


Fig. 2. Map of Kerma showing the different find contexts of the analysed artefacts.

between 1% and 10% tin (average 3.5%), except for three artefacts with 0.02% to 0.05% tin (two of these have about 1% arsenic). In the Classic Kerma artefacts, tin concentrations do not exceed 0.08% tin (except for 0.3% in KV132). The Meroitic (and possibly Napatan) artefacts contain tin at concentrations between 5% and 10% (four artefacts have only 0.05% to 0.2% tin.)

As tin does not normally occur as an accessory element within copper ores, concentrations over 0.1% can be considered the result of alloying at some point (with low concentrations often interpreted as dilution resulting from recycling and mixing). While it is possible that the smelting of stannite group minerals resulted in the direct formation of copper with low tin concentrations, this appears unlikely; the absence of tin in Kerma artefacts with similar LI ratios argues against this interpretation.

Arsenic can equally form a natural copper alloy during the smelting of arsenic-bearing copper ores, making its intentional presence difficult to evaluate. Here, the same 0.1% cut-off value is used to group samples. However, the same general division could be made using 0.5% as a cut-off value. Indeed, three broad groups of arsenic and tin alloys can be distinguished in the assemblage (beyond the four samples with arsenic and tin below 0.1%, which can be classified as “pure copper”):

- **Arsenic copper alloys without tin** ($0.1 < \text{arsenic} < 1.2\%$, $\text{tin} < 0.1\%$). Within these, a group of low-arsenic copper (0.1% to 0.3% arsenic) and arsenical copper alloys (0.7% to 1.2% arsenic) can be distinguished. No high-arsenic copper alloys are encountered in this assemblage.

- **Tin bronzes without arsenic** ($\text{arsenic} < 0.5\%$, $0.1\% < \text{tin} < 10\%$). Five of these can be considered low-tin (probably recycled) bronzes (with tin below 2%). The others have more than 4.5% tin. Tin bronzes with less than 0.1% arsenic are confined to the Meroitic period.
- **A group of “ternary alloys”** ($0.1\% < \text{arsenic} < 1.2\%$, $0.3\% < \text{tin} < 10\%$). These alloys are mainly confined to the Middle Kerma period, particularly when taking 0.5% arsenic as a cut-off value. Notably, there is no significant correlation (inverse or otherwise) between arsenic and tin concentrations.

Arsenic concentrations for these Kerma artefacts are slightly lower than those reported for Predynastic up to Middle Kingdom Egyptian alloys. Tin concentrations are overall similar to those of late Middle Kingdom to New Kingdom artefacts and are higher than those of Predynastic to Old Kingdom alloys (cf. discussion by Rademakers et al. (2021b) and references therein), with very low concentrations being relatively rare.

Leaded copper alloys are absent in the assemblage, with the exception of one artefact with 2.3% lead (Kerma period) and four artefacts with about 0.5% to 1.5% lead—below what is commonly considered a natural contaminant level from smelting copper ores (e.g., Pernicka et al., 1990). Mainly confined to the Meroitic period, these likely represent unintentional lead-bronze alloys. From the perspective of other trace elements and LI ratios, they do not stand out from other artefacts.

CET92-4



5 cm

COT90-3



5 cm

KV736



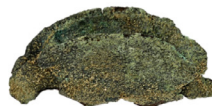
5 cm

COT114-1



5 cm

CE12



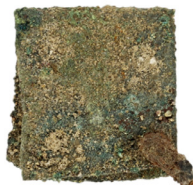
2.5 cm

CVT12-4



5 cm

CVT13



2.5 cm

KV493



5 cm

KV660



5 cm

KV496A



3 cm

Fig. 3. Selection of analysed artefacts.

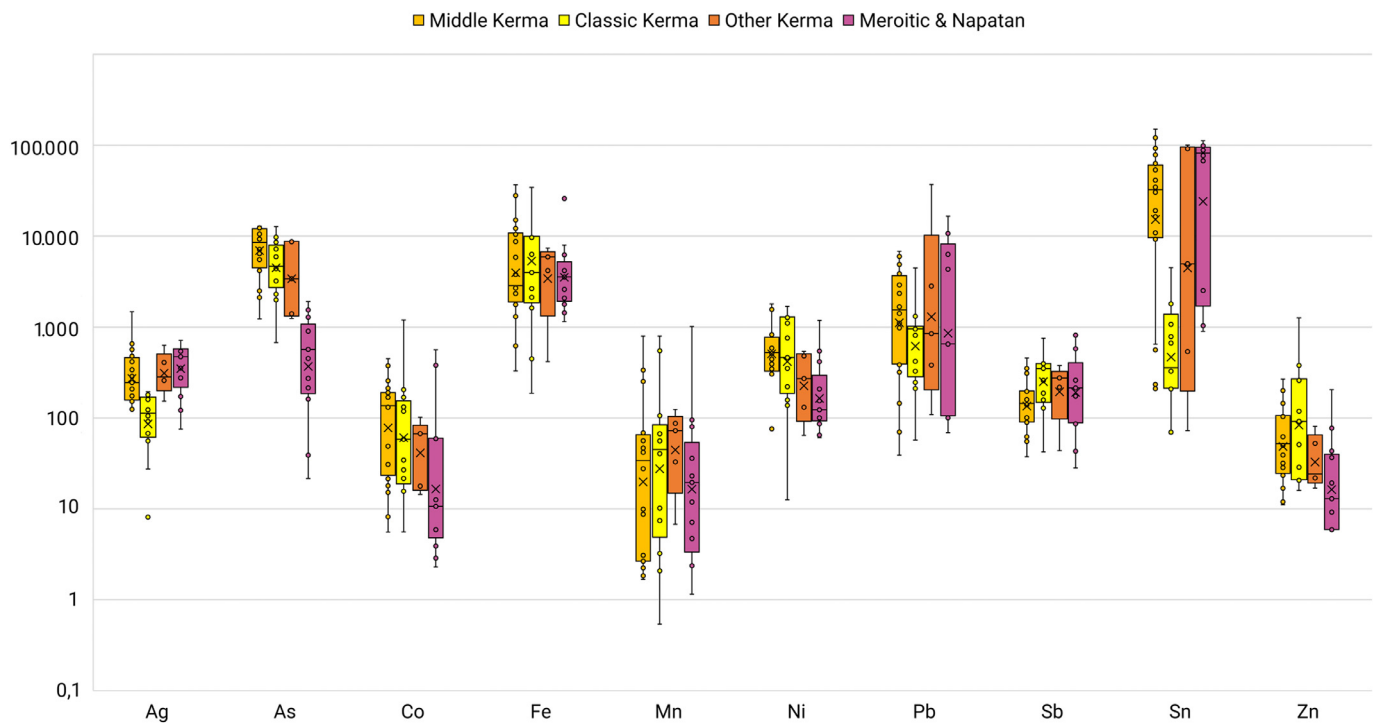


Fig. 4. Box plot of element concentrations (in $\mu\text{g/g}$, normalised to 100% copper). Comparison for Middle Kerma, Classic Kerma (including two daggers; Rademakers et al., 2021b), other Kerma, and Meroitic/Napatan copper alloys.

3.2. Trace element composition

The trace element composition for the entire assemblage is summarised by period in Fig. 4.⁸ This reveals a rather consistent trace element pattern attested in the assemblage over time. The strongest differences are noted for the Meroitic period, with slightly lower cobalt, nickel, and zinc concentrations (and a narrower selenium and tellurium variation). Overall, trace element concentrations vary between a few $\mu\text{g/g}$ and a few hundred $\mu\text{g/g}$. Only lead exceeds 1000 $\mu\text{g/g}$, varying between about 100 $\mu\text{g/g}$ and 0.3% for most periods—with the exception of a few outliers (see above). This is indicative of the exploitation of relatively pure copper ores underlying the production of these copper alloys. There is no notable distinction in terms of trace element concentrations between the three broad alloy groups discussed in the previous section. Cobalt and nickel correlate to some extent (cf. OSM: Fig. 2), with two relatively distinct groups: a low-cobalt-nickel cluster (cobalt less than 15 $\mu\text{g/g}$, nickel less than 150 $\mu\text{g/g}$) and a group with roughly correlated nickel and cobalt (nickel greater than 200 $\mu\text{g/g}$; two outliers). The former encompasses nine out of eleven Meroitic artefacts, along with artefacts from the Classic Kerma period (and one late Middle Kerma artefact), while the second group encloses most Middle Kerma artefacts. These groupings may point to the exploitation of particular ore sources. LI ratio data are discussed further below, but it can be noted here that the first cluster is associated with comparatively lower (older) LI ratios on average (some overlap exists). However, an outlier with the lowest (cobalt)-nickel content is associated with the most radiogenic LI ratios (Classic Kerma KV422C: KF_30), while the artefact with the lowest (oldest) LI ratios (Classic Kerma KV307: KF_8) falls within the second group (where somewhat elevated zinc concentration can be noted).

Arsenic does not correlate to cobalt or nickel concentrations but shows weak positive correlation to antimony, particularly for the Middle Kerma (and most Classic Kerma) artefacts. Arsenic and antimony

⁸ Corrosion effects partially distort this comparison, as a larger share of analysed artefacts from some periods (such as Classic Kerma) exhibit more significant corrosion (cf. introduction and OSM).

both further correlate to silver concentrations, again for Middle and Classic Kerma artefacts (cf. OSM: Fig. 3). This mirrors observations by Rademakers et al. (2018b, 2021b) regarding early Egyptian artefacts (see discussion below).

Lead concentrations do not correlate to other element concentrations (or LI ratios). The highest iron contents occur with strongly corroded artefacts. Excluding those, a relatively consistent iron concentration between 0.1% and 0.5% can be noted throughout the assemblage, without any clear trend over time. It is difficult to interpret such iron concentrations as linked to particular metallurgical traditions (Rademakers et al., 2020), especially when copper has been alloyed and may have been repeatedly recycled.

Trace element concentrations are compared to those of published Middle Kingdom and New Kingdom Egyptian copper alloys in Fig. 5. Copper alloys at Kerma have a highly similar trace element pattern to those of Middle Kingdom Egypt (and earlier periods; cf. Rademakers et al., 2021b). Slightly lower antimony and arsenic can be noted, while the lightly increased manganese concentrations can be attributed mainly to corrosion (see above). This trace element pattern is compatible with that of Sinai and Eastern Desert ores (cf. Abdel-Motelib et al., 2012; Pfeiffer, 2013; Rademakers et al., 2018b, 2021b) and copper produced in Sinai (Rademakers et al., 2021b)—although notable arsenic and tin concentrations are not. This means that Sinai deposits cannot be excluded as a potential copper source on the basis of elemental composition. New Kingdom Egyptian alloys tend to have higher tin and lead concentrations and slightly different cobalt, antimony, and zinc distributions, reflecting both a shift in bronze production modes and the variety of copper sources being exploited by that time (cf. Rademakers et al., 2017).

3.3. Provenance: further perspectives from LI ratios

Distinct provenance categories can be defined for ore, raw copper, and copper alloys to reflect the influence of different stages along the production chain (Rademakers et al., 2020, 2021a, 2021b). Nearly all analysed artefacts are copper alloys, so their comparison to contemporary alloys in Egypt, the eastern Mediterranean, and the Arabian Penin-

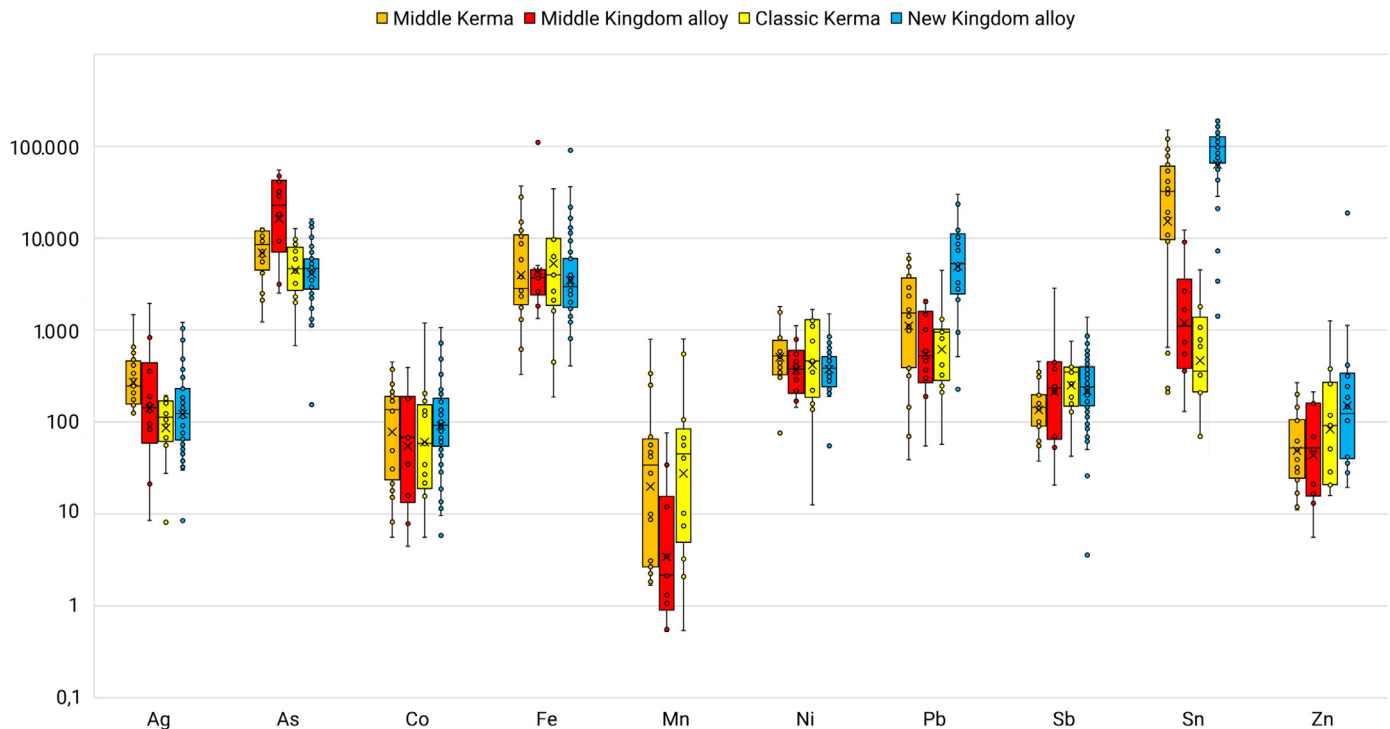


Fig. 5. Box plot of element concentrations (in $\mu\text{g/g}$, normalised to 100% copper). Comparison for Middle and Classic Kerma copper alloys to Middle Kingdom (Rademakers et al., 2021b, 10 artefacts) and New Kingdom (Odler and Kmošek, 2020, 28 artefacts; Rademakers et al., 2017, 17 artefacts; Stos-Gale et al., 1995, 16 artefacts) copper alloys. Note that trace element data are incomplete for the New Kingdom datasets, in particular with regards to zinc and lead (not reported by Stos-Gale et al., 1995; with high detection limits in Odler and Kmošek, 2020). The distributions are nonetheless in line with those attested for New Kingdom artefacts from the Royal Museums of Art and History analysed by Rademakers et al. (in preparation), not shown here.

sula is considered most instructive, although other reference data are considered too.

The elemental composition of Middle Kerma artefacts is highly similar to that of Middle Kingdom copper produced from Sinai ores in Egypt. This similarity is mirrored in the artefacts' LI ratios, as illustrated in Figs. 6 and 7. While the entire assemblage falls along a broad trend line in terms of $^{206-208}\text{Pb}/^{204}\text{Pb}$, more distinction is apparent in terms of $^{206-207}\text{Pb}/^{204}\text{Pb}$. The majority of Middle Kerma artefacts cluster along a trend line that overlaps with LI ratios for Sinai copper ores mined at Bir Nasb, Wadi Kharig, Umm Bogma, and/or Wadi Maghara during the Twelfth Dynasty and raw copper smelted from these ores, and they cluster with Middle Kingdom copper alloys analysed by Rademakers et al. (2021b). This cluster includes all waste related to the bronze casting furnace (see discussion below). The Classic Kerma dagger E.06118 (Royal Museums of Art and History, Brussels; cf. Rademakers et al., 2021b) falls along this trend line as well. Some of the Classic Kerma artefacts analysed here fall within this range too, as do a few of the Meroitic artefacts. Four of the remaining Middle Kerma artefacts (samples KF_17/25/27/28) are characterised by slightly higher LI ratios, coinciding with another group of raw Sinai copper and Middle Kingdom artefacts. Three of the remaining Middle Kerma artefacts (samples KF_19/24/26) are intermediate to these two groups, sitting closest to the first-mentioned trend line, while KV736 (KF_4) is characterised by lower LI ratios (comparable to some Protodynastic and Old Kingdom alloys, compatible with Sinai/Eastern Desert ores). Interestingly, these artefact clusters are at least partially consistent with contextual distributions (for example, KF_24/25/26/27), suggesting the use of similar material resources within some contexts.

Four Classic Kerma alloys have LI ratios similar to those found for the Middle Kerma period. KF-8 has the lowest LI ratios in the Kerma assemblage, falling roughly along the same Middle Kerma/Middle Kingdom trend line and similar to Protodynastic and Old Kingdom Egyptian copper. It can be noted that prill KV422B (KF_29), falling along

this trend line, has LI ratios indistinguishable from the blade and handle of dagger E.06118 (Rademakers et al., 2021b). Others sit just outside this range with slightly more radiogenic LI ratios (particularly thorogenic $^{208}\text{Pb}/^{204}\text{Pb}$), differing slightly from the Middle Kerma artefacts. Apart from KV422A (KF_16), these do not coincide with the circulating New Kingdom copper stock characterised at Pi-Ramesse (Rademakers et al., 2017), having slightly higher thorogenic lead. (They do not adhere to the Lavrion copper/lead ore LI ratio field either.) Rather, they partially overlap with the broad range of C-Group and New Kingdom finds from Aniba and the “intermediate group” identified at Pi-Ramesse. It should be noted, however, that these are mostly arsenical and tin bronzes, whereas many Classic Kerma artefacts discussed here are not “fresh alloys.”

The Kerma artefacts of unspecified chronology scatter across the above-mentioned groups, indicating an overall compatibility. Needle KV739 (KF_81; completely corroded) is indistinguishable in terms of LI ratios from the Middle Kingdom mirror E.04267 (Rademakers et al., 2021b) from Abydos (of similar composition but with higher lead and arsenic concentrations). The LI ratios for needle KV746 (KF_82), with a 2.3% lead concentration, are very similar to those of lead-rich C-Group axe ÄMUL 4697 (for which higher nickel and zinc concentrations are reported; Odler and Kmošek, 2020).

The Kerma-period artefacts do not reveal good consistency with other characterised sources of copper published so far. For example, there is no LI ratio overlap with Arabian Shield and Eastern Desert ore data (OSM: Fig. 4),⁹ nor with ores from Lavrion, Greece (OSM: Fig. 5). Some overlap with Omani ores and artefacts can be noted (OSM: Fig. 6), but cobalt concentrations in nearly all Kerma artefacts are below 200 $\mu\text{g/g}$ (mostly below 100 and even 10 $\mu\text{g/g}$), and nickel is be-

⁹ This concerns whole rock and lead ore data, which present some interpretational limitations with reference to copper (alloy) provenance (Rademakers et al., 2018b, 2021a).

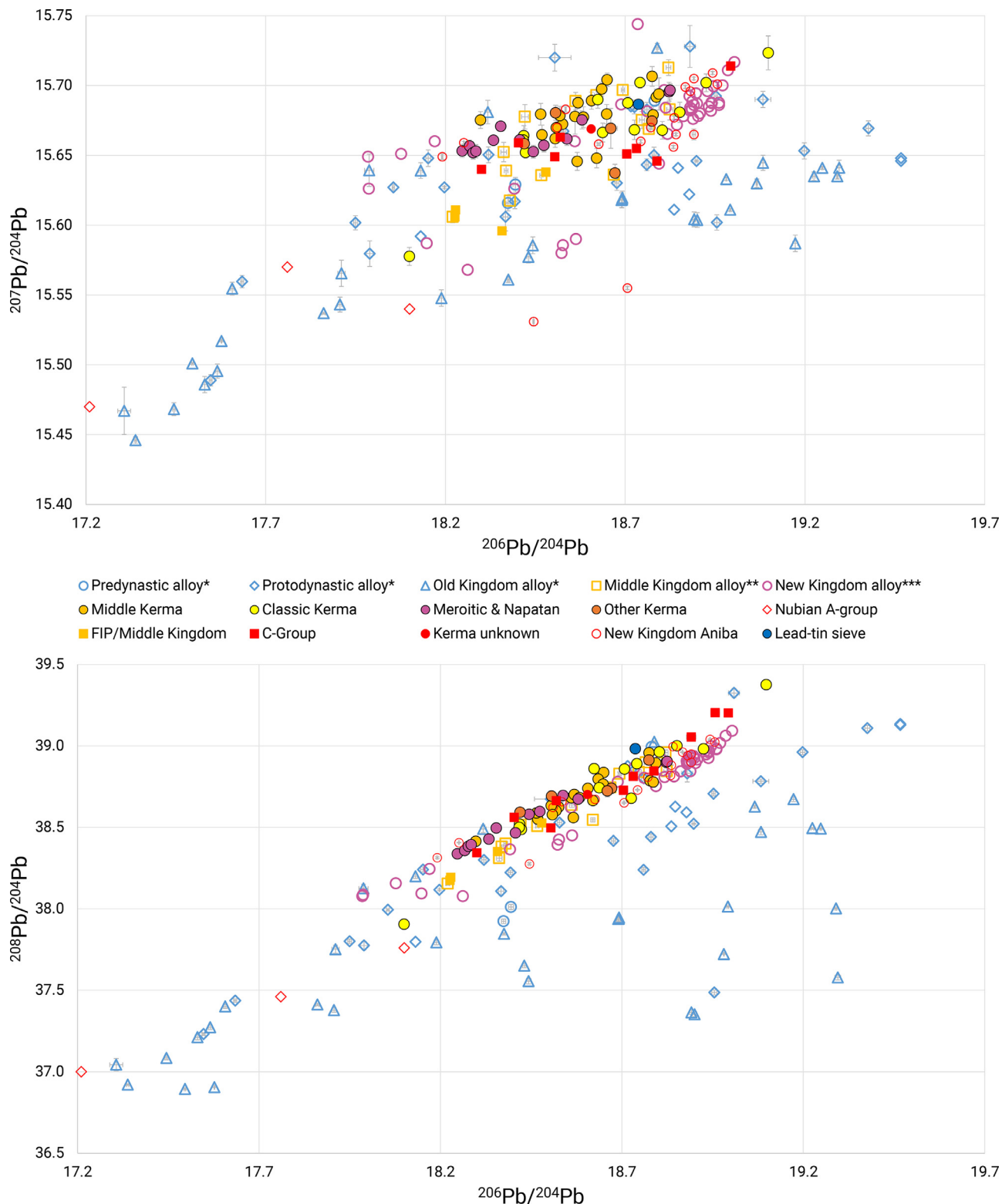


Fig. 6. Comparison of LI ratios for Kerma copper alloy artefacts (including two Classic Kerma daggers; Rademakers et al., 2021b) to published LI ratio data for ancient Egyptian copper alloys. *Predynastic, Protodynastic, Old Kingdom data: Kmošek et al., 2018 (15 artefacts), Odler et al., 2021 (10 artefacts), Rademakers et al., 2018b, 2021b (42 artefacts), Rehren and Pernicka, 2014 (13 artefacts). **Middle Kingdom data: Rademakers et al., 2021b (10 artefacts). ***New Kingdom data: Rademakers et al., 2017 (26 artefacts), Stos-Gale et al., 1995 (16 artefacts). Nubian A-Group data: Anfinset, 2010 (3 artefacts). “Kerma unknown,” FIP/Middle Kingdom, Aniba C-Group, and New Kingdom data: Odler and Kmošek, 2020 (33 artefacts). Radiogenic LI ratios not shown.

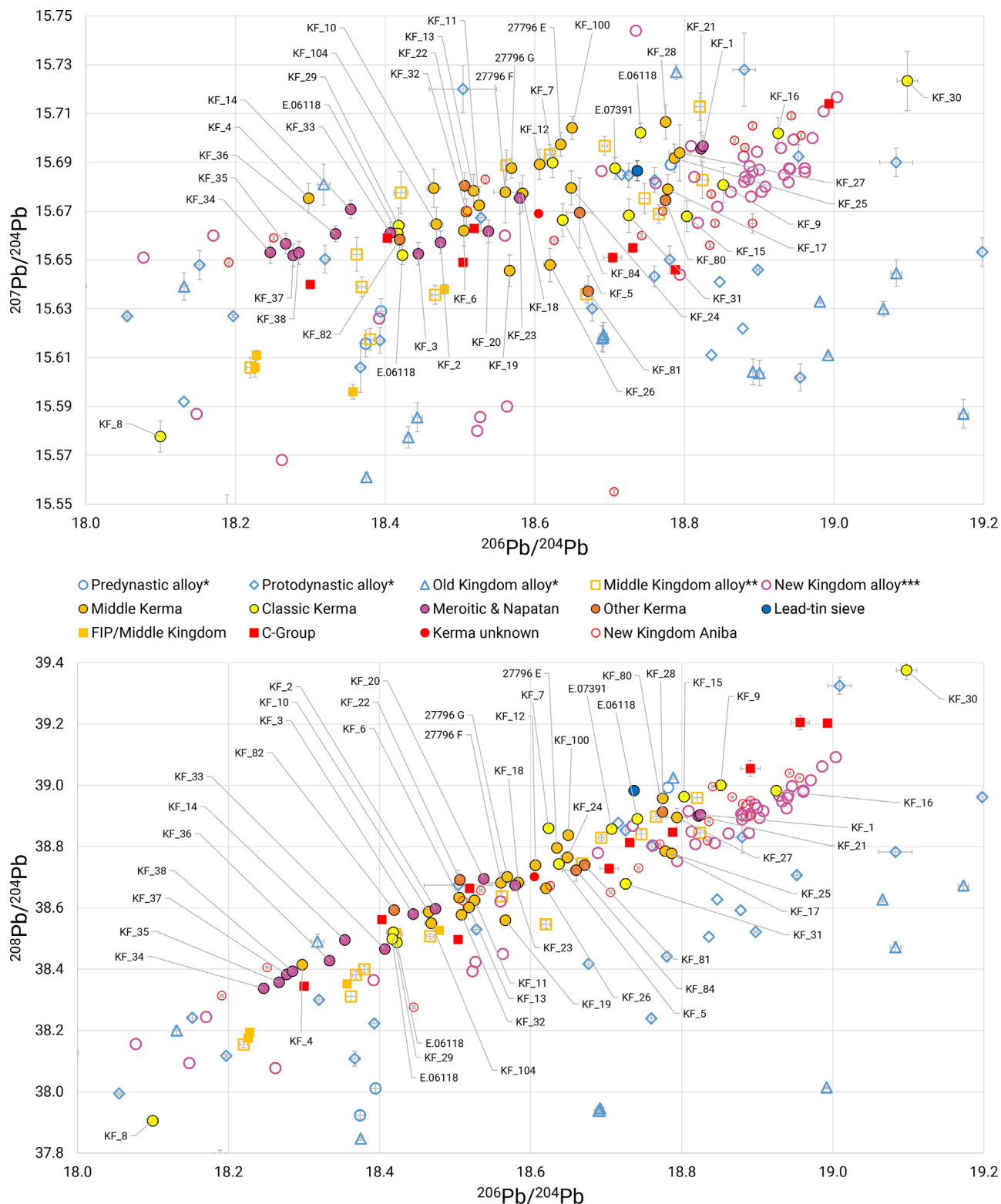


Fig. 7. Restricted LI ratio range of Fig. 5, highlighting sample labels.

low 500 µg/g (with some exceptions). In contrast, Umm an Nar- and Wadi Suq-period copper from Oman has more than 100 µg/g cobalt (averaging about 500 µg/g) and over 500 µg/g nickel (Begemann et al., 2010). Similarly, copper artefacts from the United Arab Emirates have partially overlapping LI ratios, but these artefacts generally have significantly higher nickel (mostly on the order of 0.1 wt% to a few wt%)

and cobalt (about 0.1%) concentrations (Weeks, 2003). Thus the overall geochemical match is not good. Although some influx of copper from the Arabian Peninsula cannot be excluded and such copper may be a likely constituent of the stock circulating throughout the Nile Valley (Rademakers et al., 2017), it does not appear to be the major source of metal at Kerma.

Similarly, LI ratios for ores (mainly pyrite) from Cyprus (Gale et al., 1997) are overall not consistent with Kerma artefact LI ratios, sitting below them in terms of $^{207-208}\text{Pb}/^{204}\text{Pb}$ (cf. OSM: Fig. 7). Nonetheless, marginal overlap can be noted with the Limni axis and Limassol Forest ranges for one “other Kerma” and two Middle Kerma artefacts. However, it makes more sense to interpret these in light of the Kerma artefact assemblage as a whole (see above), as their composition does not indicate them to be outliers and no Cypriot artefacts with comparable composition are known. It can be noted that LI ratios for Kerma blade ÄMUL 3791 sit at the very edge of the Limassol Forest ore range. While Odler and Kmošek (2020: 138, 147) consider a Cypriot origin to be most likely for this blade (an overlap with the Limni axis is postulated, but LI ratios for the closest pyrite sample differ by 0.1% in $^{208}\text{Pb}/^{204}\text{Pb}$),¹⁰ Egyptian and Kerma copper provide a much better point of comparison.¹¹

The Arabah Valley (Israel, Jordan) was another important source for Bronze Age metal, with Timna and Faynan as its main mining zones. The LI ratios for Kerma artefacts are not consistent with those for copper ores from Timna and Faynan (cf. OSM: Fig. 8) nor with those for Bronze/Iron Age copper ingots from Timna, Faynan, and Levantine sites. However, some overlap can be noted with a specific part of the Faynan ore range: the massive brown sandstone (MBS) formation (Hauptmann, 2007). Because they are relatively “pure” ores, it may be difficult to distinguish copper smelted from Faynan MBS ores from Sinai copper in terms of either LI ratios or trace element concentrations. However, the majority of mining evidence for these deposits dates to the Roman period (for example, mining at Wadi Abiad and Qalb Ratiye and smelting at “Faynan 1”; Hauptmann, 2007).¹² Thus the Arabah Valley is similarly unlikely to have been a major source of copper for the Kerma-period artefacts.

Four closely clustering Meroitic artefacts do fall just within the currently known LI range for Timna copper ores. These are part of a group of six rings and attachments (COT79/6) from the Western Necropolis that are compositionally similar as well. Two rings (KF-37/38) have identical LI ratios and elemental compositions (apart from slightly different tin concentrations). The other four samples have lower (by five times) lead concentrations. KF-33 is closest in composition but differs most in

¹⁰ The proposed Cypriot origin for some New Kingdom Aniba artefacts (Odler and Kmošek, 2020: 141) is equally or more problematic. For example, artefacts ÄMUL 2191 and ÄMUL 2142 fall outside the Solea axis and Larnaca (Sha) axis LI ranges, respectively. Artefact ÄMUL 2167 does sit on the edge of the Limassol Forest range but is similar to Kerma copper alloys and New Kingdom “intermediate copper” from Pi-Ramesse (Rademakers et al., 2017). Again, there is no specific evidence indicating a Cypriot origin (for example, analysed Limassol Forest copper ores have high cobalt and nickel concentrations; Stos-Gale et al., 1997). Nonetheless, Odler and Kmošek (2020: 155) assert that it was “made of Cypriot ore.” ÄMUL 2178 is similarly stated to have been “made solely of Cypriot ore,” yet arguments against a Cypriot provenance for a Pi-Ramesse dagger with nearly identical LI ratios are provided by Rademakers et al. (2017). Such positive attributions are thus in need of further nuance (see also Rademakers et al., 2021a).

¹¹ If links with Cyprus are to be proposed, comparisons between Kerma-period artefacts and datasets on Early and Middle Cypriot (and Late Cypriot I) copper alloys may be more instructive. While many are consistent with Cypriot ore deposits (and thus not with Nile Valley copper alloys), a large group of these artefacts is not. Many artefacts from Cyprus not matching Cypriot ores equally overlap with the Kerma (and Egyptian) copper alloy LI ratio range. Yet there are no Pb concentration data available for most of these artefacts, and their trace element concentrations are variable. Stos-Gale and Gale (2010) interpret them as most likely produced from Anatolian, Cycladic, and Western Mediterranean copper ores. Thus the available evidence for a more local origin of Egyptian/Nubian copper provides a much better interpretation hypothesis than suggestions of “foreign” copper making its way (via Cyprus) into the Nile Valley in large quantities.

¹² Note that the LI ratios for Roman slag JD-1/9 (Hauptmann et al., 1992) are consistent with DLS ores (Hauptmann, 2007: 213–15, Figure 6.45) and that most Roman mines were worked between the second and fifth centuries CE (Hauptmann et al., 1992).

terms of LI ratios (falling outside the known Timna range). The other three are more similar to each other (with slightly higher arsenic, antimony, phosphorus, and sulphur concentrations) and scatter across the limits of the Timna LI range. As these artefacts fall outside the LI ratio trend lines observed for earlier Kerma copper, and the Meroitic artefacts differ in their elemental composition overall (lower arsenic, zinc, cobalt, and nickel concentrations), they most likely represent different copper sources. The Arabah Valley is a valid candidate, but other Sinai deposits, or a combination of sources, are possible too. Indeed, out of the Levantine ingots analysed by Yahalom-Mack et al. (2014), the Bir Nasb¹³ copper ingot has identical LI ratios to KF-36 (similar to some Timna ingots). This group of artefacts is revisited in the discussion below.

Out of the remaining seven Meroitic (including two possibly Napatian) artefacts, rod KF_14 is isotopically very similar to the above-mentioned group but is characterised by lower silver and antimony and higher cobalt, nickel, and zinc concentrations, implying a different geological provenance. The other six artefacts sit outside the Timna range. (Four of these have elevated lead content compared to the other Meroitic artefacts, most outspoken in KF-1 and KF-21, which are isotopically indistinguishable.) As noted above, their LI ratios overlap with those of Middle and Classic Kerma artefacts. Furthermore, they broadly overlap with the Faynan MBS ore range (Hauptmann, 2007). However, there are no good comparatives to suggest the import of Faynan copper during the Meroitic period here,¹⁴ although this cannot be formally excluded given the compositional variation reported for the few Roman-period samples and the scale of Roman mining throughout Faynan (including the reopening of older mines and the large mines at Umm el-Amad for which no LI ratios are currently available; Hauptmann, 2007). Copper for these Meroitic artefacts may thus derive from Sinai or Eastern Desert deposits, Faynan, or the Arabian Peninsula.¹⁵

3.4. Lead-tin artefact

The Meroitic-period “sieve” artefact (COT 90/3) is a lead-tin alloy. It is dominated by lead with about 8.5% tin.¹⁶ Trace element concentrations are low (silver and bismuth below 100 $\mu\text{g/g}$, 130 $\mu\text{g/g}$ sulphur, and 240 $\mu\text{g/g}$ antimony), although about 0.1% copper can be noted.

¹³ Bir Nasb was an enormous mining and smelting zone in Sinai (e.g., Abdel-Motilib et al., 2012), but so far only two slag samples and one copper ingot have been geochemically characterised.

¹⁴ Concentrations of silver and antimony (relative to copper) in copper ores from the Roman mines at Wadi Ratiye (Hauptmann, 2007: Table A.1) are not compatible with the Meroitic artefacts. Two Roman copper alloy artefacts from the Abu Dhubbaneh smelting site (Hauptmann, 2007: Table A.17; LI ratios are not reported) have notably elevated silver and antimony concentrations compared to Faynan copper artefacts from other periods, but this is not reflected in Roman copper and slag from Faynan, which in turn has much higher cobalt concentrations than the Meroitic artefacts (Hauptmann, 2007: Table A.20).

¹⁵ While LI ratios for most Early Iron Age copper alloys from Tayma, in northwestern Arabia (Renzi et al., 2016), do not overlap with the Kerma assemblage, those for three artefacts (TA8901, TA16061, TA16059) overlap with the main Middle Kerma cluster. (They are not plotted, as they fall outside this paper’s chronological scope.) LI ratios for most (late) Roman crucible remains from Tayma (Liu et al., 2015) overlap with those of some Middle and Classic Kerma artefacts, as well as some Middle and New Kingdom Egyptian artefacts (with TA-5675 better resembling Old Kingdom artefacts with lower LI ratios), but not with the Meroitic artefacts presented here. This could suggest the existence of a shared supply network for northwestern Arabia and the Nile Valley during the Bronze Age, involving copper from (southwestern) Arabia and/or the Nile Valley. However, crucible LI data should be treated with caution (Rademakers et al., 2017) and are therefore not included in LI ratio plots here. Further analysis of metal remains from Arabia is needed to better illuminate this connection.

¹⁶ Dilute nitric acid was used to dissolve this lead-dominated alloy, which may result in lowered tin recovery due to its poorer solubility. The original tin concentration may thus be slightly higher.

Few contemporaneous artefacts with similar composition have been published, although lead-tin alloys were known at the time. For example, Roman pewter ingots usually had much higher tin concentrations (e.g., Beagrie, 1989, Hughes, 1980) while solders often had lower tin concentrations (e.g., Gomes et al., 2016). Gener et al. (2014) note that solder of about one part tin to three parts lead was used by the Romans, as described by Pliny (e.g., Paparazzo, 1994), although tin was diluted during soldering and the later recycling of soldered lead objects. No comparatives from the Nile Valley have been published so far.

The sieve's LI ratios (cf. OSM: Figs. 9 and 10), representing those of the lead component in the alloy, fall within the broad range of Kerma (and Egyptian) copper alloys, although with notably higher $^{208}\text{Pb}/^{204}\text{Pb}$. While they are broadly consistent with the Sinai ore range, these concern copper ores and no (exploitation of) Sinai lead ore has been reported. Galena mined in the Eastern Desert, for example at Gebel Zeit (Castel and Soukiassian, 1989), has not been extensively characterised in terms of LI ratios but can be expected to conform to Eastern Desert–Arabian Shield data (Shortland, 2006), which (like Egyptian and Nubian kohl data)¹⁷ do not match those of the lead-tin sieve. LI ratios of four lead weights from Amarna (Shortland, 2006) and lead sinkers from Pi-Ramesse (unpublished) are distinct from those of the sieve (both New Kingdom; the former match Lavrion lead ore LI ratios while the latter reflect multiple sources). These equally differ from LI ratios measured for Late Period up to Roman-period leaded bronze and lead artefacts from Naukratis (Masson-Berghoff et al., 2018), Qubbet el-Hawa (Schwab and Willer, 2016), Kawa, Sanam abu Dom, and Memphis (Fleming, 1982).

The sieve's LI ratios are not consistent with lead ores from Lavrion or Thasos (Greece), which were likely sources of lead for Egypt during the New Kingdom and/or Late Period as attested by the above-mentioned lead and leaded bronze finds. Its LI ratios are not consistent with characterised Sardinian, Iranian, and Turkish lead ores (see full reference data in OSM) either, but overlap can be noted with lead ores from Siphnos (Cyclades), another likely lead source for Late Period Egypt. However, mining and smelting evidence from Siphnos is limited from the sixth to fifth century BCE onwards (Matthäus, 1985; Pernicka and Wagner, 1985). This makes it a less likely source for lead in Meroitic Kerma, although it cannot be excluded formally.

LI consistency can equally be noted with (eastern/central) Rhodope (Bulgaria) lead ores, which were exploited during the early Roman period (cf. Kuleff et al., 1995, 2006). Furthermore, the sieve's LI ratios match those of Roman lead ingots, which are consistent with the Cartagena-Mazzarón ore district (Spain) (Trincherini et al., 2009), while a few Punic and Roman lead artefacts from Carthage (Tunisia) have similar LI ratios too (Farquhar and Vitali, 2009). The sieve's LI ratios differ from Roman lead artefacts from Germania (Bode et al., 2009) and leaded copper alloy coins from Jordan (Birch et al., 2019).

4. Discussion

For the Early Kerma period, no data are currently available. LI ratios for three Middle and Terminal A-Group Nubian artefacts (dated about 3400–2900 BCE) represent rather old geological deposits (Anfinset, 2010; Nordström, 1972) and do not match those of any Kerma copper artefacts presented here. However, their LI ratios fall within the range of Protodynastic and Old Kingdom Egyptian copper alloys. The A-Group artefacts have very low (less than 100 $\mu\text{g/g}$) iron concentrations and notable arsenic concentrations, similar to some Pre- and Protodynastic artefacts reported by Rademakers et al. (2018b).

¹⁷ So far, no evidence has been published to support the extractive metallurgy of lead from Eastern Desert ores (for example, at the extensive galena mines of Gebel Zeit), yet more extensive research remains to be conducted. At any rate, these mines were exploited for minerals used as kohl. Parallel to the study of lead provenance throughout the Nile Valley, the provenance of kohl across Egypt and Sudan (and its entangled transmission of cosmetic practices; Walsh, 2020) remains to be studied in further detail.

This suggests that they may have been produced from a similar geological source (as argued for two Protodynastic artefacts from Faras; Rademakers et al., 2018b). While this could indicate a shared origin for early metals throughout the Nile Valley, it is equally possible that ore deposits in Egypt and Nubia yielded similar copper compositions independently. This cannot be resolved until Nubian copper sources are better characterised, but similarity in elemental concentrations (including arsenic) and LI ratios may argue more strongly for exchange between A-Group and Naqada people, as indicated by other material culture evidence (e.g., Edwards, 2004).

Overall, Kerma artefacts are very similar to Egyptian copper alloys in terms of both elemental composition and LI ratios, which could be suggestive of a shared copper provisioning network. This network might well extend to the Arabian Peninsula, at least for certain periods of time. Therefore it could be proposed here that copper primarily produced in Egypt made its way to Kerma. Comparatively lower concentrations of arsenic and antimony (and cobalt and zinc, to a lesser extent) in Kerma artefacts could then be interpreted as minor losses through recycling¹⁸ or differences in arsenic alloying.¹⁹ It must be emphasised, however, that a strong research bias has favoured the characterisation of Egyptian metalwork and mining zones so far (even if these remain to be characterised in greater detail), making it difficult to assess Nubian copper provisioning on its own terms. Indeed, other primary sources of copper may have been exploited, for example in Nubia's Eastern Desert and Darfur (Herbert, 1984; Master et al., 2016),²⁰ resulting in copper with highly similar characteristics given the shared geological background. Thus it may be impossible to distinguish locally produced copper from “Egyptian” copper.²¹ In such a scenario, arsenic levels in the Kerma artefacts could reflect directly smelted natural alloys or secondary alloying and mixing/dilution processes. Contrary to the situation in Old and Middle Kingdom Egypt, where geological and smelting evidence points to active arsenic alloying (Rademakers et al., 2018b, 2021b and references therein), these scenarios cannot be further elaborated for Kerma. Further investigations on Nubian mining zones, as well as the characterisation of copper alloy artefacts and production waste from sites across modern-day Sudan and the Arabian Peninsula, are required to test these hypotheses.

¹⁸ Although iron concentrations are not lower, which may argue against such an interpretation.

¹⁹ Whereby antimony may have been associated with arsenic. See discussion by Rademakers et al. (2018b, 2021b).

²⁰ However, (copper) ores from the Nubian Eastern Desert are expected to be geochemically similar to those of the Egyptian Eastern Desert (Nubian Shield) and those of Saudi Arabia and Yemen (Arabian Shield) (Shortland, 2006; Weeks et al., 2009). If so, these ores may be less likely source candidates (cf. OSM: Fig. 9).

²¹ Davey et al. (2021) highlight the possible exploitation of an arsenic-nickel-rich copper ore at the Middle Kingdom settlement at Buhen. This may represent another ore type available in Nubia, although it could not be identified with confidence in this assemblage. It can be noted that CET111/2 (KF.19) comes closest with about 0.7% arsenic and 0.2% nickel (and notably 0.1% gold), but taking into account its LI ratios, a distinct ore source cannot be defined. El Gayar and Jones (1989a) discuss a copper ore fragment from the Old Kingdom town at Buhen with an elevated gold concentration and overall low trace elements, with the exception of 2.3% zinc and 0.1% silver (arsenic is not reported). Its source deposit could not be identified confidently. Umm Semiuki was dismissed due to its location far from Buhen, although more recent analysis suggests that elevated zinc (and possibly silver) concentrations may occur there (see Rademakers et al., 2021b: 25). El Gayar and Jones (1989b) suggest that the ore fragment may represent a distinct type available for copper production in northern Sudan, as reflected in a metal prill at Buhen. The strongly elevated gold concentration (about 0.5%) in Kerma prill KV742 (KF.24) might reflect the use of such an ore, but its LI ratios are not distinctive. Thus the elevated gold content in this prill could equally reflect a strong contamination from alloying with alluvial cassiterite or the recycling of gilded artefacts (cf. Rademakers et al., 2017).

Regardless of the primary provenance of the copper, it is apparent from this study that secondary metallurgy at Kerma played an important role. This is reflected rather spectacularly in the bronze plate casting furnace and less conspicuously in the important tin concentrations already appearing during the Middle Kerma period. While the timing for the adoption of tin alloying in Egypt is not that well constrained (Rademakers et al., 2021b), it is well attested during the Middle Kerma period. Indeed, tin concentrations in the Middle Kerma alloys are relatively higher than those of most Middle Kingdom alloys, while arsenic concentrations are relatively lower (Fig. 5). This may suggest independent traditions in secondary metallurgy existed along the Nile Valley, whether raw copper sources differed or not.

From the perspective of arsenic, the compositional pattern for the Middle Kerma ternary alloys can be explained in two main ways. On the one hand, arsenic may not have been recognised as an alloy component of copper, with all “base copper” having a (natural) arsenic content ranging between 0.1% and 1.2%. On the other hand, copper alloys of arsenic and tin may have been used interchangeably as “bronze”—possibly without a distinction between the two (at all times). As the majority of ternary alloys have more than 0.5% arsenic and available geological data argue against natural arsenical copper alloys, the latter appears a more likely explanation (see discussions of Egyptian copper alloys in Rademakers et al., 2021b), but this remains to be explored further (see above). The Middle Kerma casting furnace remains appear to result from intentional arsenic and tin alloying, with bronze composition ranging from 0.5% to 1.1% arsenic and 2.5% to 7.5% tin. Furthermore, the presence of less than 2.5% tin in combination with 0.5% to 1.2% arsenic suggests the existence of “recycled ternary alloys” as early as the Middle Kerma period. If recycling may be considered a key facet of metal provisioning in the Nile Valley, with “Egyptian metals” possibly comprising part of the supply at Kerma, lower concentrations of both arsenic and tin are likely reflections of flexible recycling and alloying practices. Higher tin concentrations amongst the casting spills and objects (for example, about 10% in bracelet KV746 and uraeus KV493) indicate that active alloying did take place at Kerma and that alloys were surely recognised by the highly skilled craftspeople active in this region.

For the Classic Kerma period, only arsenical copper alloys are reported, while tin bronze is absent from the assemblage. Nonetheless, tin concentrations of about 0.1% to 0.3% likely reveal the recycling and mixing of tin bronze during this period. It is expected that higher tin bronzes equally existed at Kerma during this period, yet surprisingly little analytical data are currently available to validate this. The blades of two Classic Kerma daggers analysed by Rademakers et al. (2021b) are made of low arsenical copper, while Vercutter et al. (1960) report on the analysis of a Classic Kerma dagger (from Grave K.1620, subsidiary to Tumulus XVI; Bonnet, 2000: 16–21) made of tin bronze with minor lead and arsenic, and traces of nickel, silver, antimony, and bismuth (concentrations are not specified). Cowell (1987) further reports on the composition of two (probably Classic) Kerma daggers from the British Museum (EA55442 and EA55443), with the former containing 1.4% arsenic and 0.4% tin (its rivet has only 0.6% arsenic; see observations by Rademakers et al., 2021b) and the latter containing 0.8% arsenic, 8.9% tin, and 1.5% lead. Some Classic Kerma artefacts analysed by Dunham (1943) have percentage levels of tin too. It thus appears that Classic Kerma dagger alloy compositions varied significantly, perhaps reflecting differences in functionality, personal expression (see Walsh, 2021 on metal vessels), or alloy availability. Therefore the lack of tin bronzes in the presented Classic Kerma assemblage, which includes small unalloyed copper prills, fragments, and rods, may simply be a sampling artefact. While it is possible that tin was not widely used for smaller object types and was mainly reserved for prestige items (such as daggers), a wider dataset is required to assess this more confidently. Current data are similarly insufficient to speculate on the supply chain of tin for Kerma (as part of long-distance exchange networks or more local production from Eastern Desert cassiterite; cf. Rademakers et al., 2018a) and its possible disruption over time.

While there is a significant time gap between the Kerma and Meroitic periods, for which no analytical data are currently available, arsenic content is observed to decrease over time, with tin bronzes dominating the Meroitic assemblage. This may be explained by the recycling of “old copper” during tin alloying, whereby arsenic is progressively lost over time. However, the very low (less than 0.1%) arsenic concentrations in several artefacts argue against this and point to the alloying of fresh copper with tin at that time. Indeed, there appears to be no shift towards strongly clustered LI ratios, as would be expected for a system relying heavily on recycling. Rather, the spread in LI ratios implies an influx of fresh copper. As discussed above, the combined evaluation of LI ratios and elemental compositions suggests that multiple copper sources likely underlie the production of these Meroitic bronzes. This may include the continued exploitation of copper sources attested during the Kerma period (whereby the alloying with arsenic is progressively abandoned in favour of tin alloying) as well as possible copper imports from the Arabah Valley and Arabian Peninsula.

These observations do not reveal where the alloying took place. In this regard, it is instructive to consider the bronze casting remains. For these five samples, there are notable differences in both arsenic and tin concentrations. Two (MAH 27796-F/G) are nearly identical in terms of LI ratios and have identical trace element concentrations (silver, gold, cobalt, nickel, lead, and antimony), while arsenic and tin (and iron) vary only slightly. These most likely represent two spills from a single production event (possibly from the crucible they were found associated with).²² The LI ratios of MAH 27796-E and KF-100 are relatively similar (but not identical), as are their trace element patterns. Finally, a copper prill found lower in the furnace rubble again has different LI ratios and a very slightly different trace element pattern.

These minor differences, particularly in terms of arsenic and tin concentrations, imply that at least three crucible batches are attested here—which makes perfect sense considering the small crucible volumes relative to the cast plate volume, as discussed in detail by Verly et al. (in preparation). The high similarity in trace element composition, however, indicates the likely use of a single copper source. The discrepancy in terms of LI ratios and arsenic and tin concentrations between these batches suggests that variable amounts of tin (and arsenic?) were being added to each charge, possibly shifting the LI ratios.²³ This would argue for alloying being performed on the spot, as required for the particular casting goal. Analysis of the crucible remains is expected to clarify this further.

Six Meroitic samples are part of a composite artefact (COT79/6) consisting of eight rings attached to a largely disintegrated wood fragment. Four rings were made of copper and apparently cast in a ring shape, while the other four are made of tin bronze (as identified by handheld XRF on-site) and appear to be rods hammered into a ring shape. The copper rings were fastened using copper attachments (folded rods), while the bronze rings were held in place with iron attachments (three are preserved) to create two different colour schemes. A larger bent bronze rod was associated with this composite artefact. These samples form a broad cluster in terms of LI ratios and have very similar elemental compositions. Three out of six consist of unalloyed copper (less than 0.3% tin), while three are tin bronzes (7% to 10% tin). The compositions of two bronze rings (KF_37–38) are identical within analytical error and may reflect a single crucible batch. Unalloyed attachment KF_35 and ring KF-36 (one folded around the other) are almost identical in terms of elemental composition but have distinct LI ratios. Bent and folded

²² Similar and even more pronounced variations in arsenic and tin concentrations between spills of a single crucible charge were observed by the authors during experimental casting (unpublished data).

²³ It can be noted that all samples lie on a trend line in LI space (cf. OSM: Fig. 11), roughly arranged according to tin and lead concentration. The LI range attested for the casting remains is similar to that of several other Middle Kerma artefacts; seven samples in particular (KF-6/10/11/12/13/18/32) fall along the same trend line (see section 3.3).

rods KF_33 and KF-34 have highly similar elemental composition (except for their 0.1% and 10% tin) but significantly different LI ratios. It can be suggested that these pieces were all made from the same base copper. The three bronze parts have slightly lower arsenic, cobalt, antimony, phosphorus, and sulphur concentrations compared to the unalloyed copper ones, which may be explained by minor losses during melting and alloying. A trend line through the three bronzes differs slightly from a trend line through the unalloyed copper (higher with reference to $^{207}\text{Pb}/^{204}\text{Pb}$, lower with reference to $^{208}\text{Pb}/^{204}\text{Pb}$). This may suggest a relative shift in LI ratios through the alloying process, given their low lead concentrations.²⁴ (A minor increase in lead concentration can be noted for two of the bronze rings.) The low but notable tin concentrations in the unalloyed copper may suggest that an existing artefact was recycled or that a contaminated crucible was used for melting raw copper. Alternatively, a copper source with elevated tin concentrations may have been used, but this is not compatible with the suggested Sinai/Faynan/Arabian copper sources.

Beyond tin bronzes, leaded bronzes became widespread from the late New Kingdom onwards in Egypt and are equally attested in Nubia—at Late Period Kawa and Sanam, for example (Fleming, 1982). While absent from the sampled artefacts held at the excavation house, several Meroitic leaded bronzes were identified (with handheld XRF) within the Kerma and Geneva museum collections (for example, bowls MAH 024888 and MAH 027778). Leaded bronze was thus in use at Kerma during the Meroitic period. Furthermore, the use of lead at Kerma is directly attested in this assemblage in the form of a lead-tin sieve. This sieve's lead, possibly already mixed with tin and perhaps representing a mixture of different lead sources, may have been obtained through Roman trade networks.²⁵ Less likely, (de-silvered) lead from Siphnos may have travelled down the Nile Valley. Thasos lead, attested in Late Period contexts such as Qubbet el-Hawa and Naukratis, appears not to have been used in the production of this artefact. More extensive analysis of lead and leaded materials from Egypt and Nubia may change this picture, however, as lead use in the Nile Valley remains poorly understood. The targeted analysis of leaded bronzes (Rademakers et al., in preparation) and lead-rich glass (e.g., Spedding, 2022),²⁶ for example, can play an important role in illuminating the provenance of this widely used metal.

5. Conclusion

This paper presents the first diachronic overview of copper alloy compositions in circulation at ancient Kerma. A gradual replacement of arsenical copper by tin bronze over time is noted, although these alloys may have been used interchangeably and mixed as part of a flexible alloying strategy as early as the Middle Kerma period. Overall, a close compositional resemblance is noted between copper alloys at Kerma and those encountered over the same time frame downstream in Egypt. It is difficult to ascertain the extent to which production and consumption systems in Nubia and Egypt were entwined, particularly given the scarcity of research into ancient mining and metallurgy in Nubia. It is possible that highly similar alloys resulted from a largely independent exploitation of geologically similar resources. However, it is equally possible that a kind of metallurgical *koiné* existed throughout the Nile Valley, with raw materials, production techniques, and perhaps craftspeople moving and exchanging at varying intensities over time. More extensive analysis of metal artefacts and production remains, alongside dedicated excavation of workshops and well-conceived experimentation, is essential for obtaining a more holistic understanding of ancient metal

²⁴ For example, Begemann et al. (2001) and Rademakers et al. (2017) discuss the possibility of minor lead being introduced as a tin contaminant during alloying, thus shifting the LI ratios between bronze and copper.

²⁵ The possible use of Faynan copper during the Meroitic period could not be ascertained, but its import through Roman trade networks can be imagined.

²⁶ Six lead-rich glass artefacts from Faras, Gabati, and Meroe have similar LI ratios to those of the sieve.

production at Kerma. While it is too early to draw firm conclusions at this point, it is clear that investigations of metallurgical technology in Nubia can illuminate broader issues, such as technological exchange, innovation, and ancient trade networks, on a much wider scale.

Declaration of Competing Interest

The authors declare that they have no known competing financial interests or personal relationships that could have appeared to influence the work reported in this paper.

Acknowledgments

We want to thank the National Corporation for Antiquities and Museums (NCAM) of the Republic of the Sudan for giving us the opportunity to analyse this unique assemblage. We particularly thank Dr. Abd el-Rahman Ali, former director of NCAM; Dr. El-Hassan Ahmed, director of excavations; and inspectors Abd el-Magid Mahmud and Abd el-Hay Abd el-Sawy for their help during the exportation procedures. Analytical research was supported by the Michela Schiff Giorgini Foundation and the KU Leuven Centre for Archaeological Sciences.

We are grateful to Béatrice Blandin and Bernadette Rey-Bellet, curator and conservator at the Musées d'art et d'histoire de Genève, for their assistance in sampling the casting spills and studying the Kerma artefacts held at the collection. We also want to thank Katia Novoa, scientific contributor, and the museum's technical staff for their precious help.

We thank Elvira Vassilieva for performing the ICP-OES analyses and Kris Latruwe for performing quantitative Pb determination using ICP-MS and performing Pb isotopic analysis using MC-ICP-MS at Ghent University. We thank Juliet Spedding for sharing the LI ratio data on the Nubian glass artefacts before publication and Thilo Rehren, Edgar Pusch, and Zofia Stos-Gale for sharing the unpublished Pi-Ramesse lead data.

We are grateful to the editor and three anonymous reviewers for their constructive comments, which helped improve this manuscript.

Supplementary materials

Supplementary material associated with this article can be found, in the online version, at doi:10.1016/j.aia.2022.01.001.

References

- Abdel-Motelib, A., Bode, M., Hartmann, R., Hartung, U., Hauptmann, A., Pfeiffer, K., 2012. Archaeometallurgical expeditions to the Sinai Peninsula and the Eastern Desert of Egypt (2006, 2008). *Metalla* 19, pp. 3–59.
- Anfinset, N., 2010. *Metal, Nomads and Culture Contact: the Middle East and North Africa*. Routledge, London.
- Beagrie, N., 1989. The Romano-British pewter industry. *Britannia* 20, pp. 169–191.
- Begemann, F., Hauptmann, A., Schmitt-Strecker, S., Weisgerber, G., 2010. Lead isotope and chemical signature of copper from Oman and its occurrence in Mesopotamia and sites on the Arabian Gulf coast. *Arab. Archaeol. Epigr.* 21, pp. 135–169.
- Begemann, F., Schmitt-Strecker, S., Pernicka, E., Lo Schiavo, F., 2001. Chemical composition and lead isotope of copper and bronze from Nuragic Sardinia. *Eur. J. Archaeol.* 4, pp. 43–85.
- Birch, T., Orfanou, V., Lichtenberger, A., Raja, R., Barfod, G., Leshner, C.E., Schulze, I., Schulze, W., 2019. From nummi minimi to fulūs - small change and wider issues: characterising coinage from Gerasa/Jerash (Late Roman to Umayyad periods). *Archaeol. Anthropol. Sci.* 11, pp. 5359–5376.
- Bode, M., Hauptmann, A., Mezger, K., 2009. Tracing Roman lead sources using lead isotope analyses in conjunction with archaeological and epigraphic evidence - a case study from Augustan/Tiberian Germania. *Archaeol. Anthropol. Sci.* 1, pp. 177–194.
- Bonnet, C., 1986. Un atelier de bronziers à Kerma. In: Krause, M. (Ed.), *Nubische Studien. Tagungsakten der 5. Internationalen Konferenz Der International Society For Nubian Studies*, Heidelberg, 22–25. September 1982. Verlag Philip Von Zabern, Mainz, pp. 19–22.
- Bonnet, C., 2000. *Édifices Et Rites Funéraires à Kerma*. Errance, Paris.
- Bonnet, C., 2004. *Le Temple Principal De La Ville De Kerma et Son Quartier Religieux*. Errance, Paris.
- Bonnet, C., 2014. *La Ville De Kerma. Une capitale Nubienne Au Sud De L'égypte*. Favre, Lausanne.
- Bonnet, C., 2019. *The Black Kingdom of the Nile*. Harvard University Press, Cambridge, MA.

- Bonnet, C., Valbelle, D., Marchi, S., 2021. Le jububier, Ville Sacrée Des Pharaons Noirs. Khéops, Paris.
- Castel, G., Soukiassian, G., 1989. Gebel El-Zeit I. Les mines De Galène (Egypte, Ile Mil-lenaire av. J.-C.), FIFAO 35. Institut Français de Archéologie Orientale, Cairo.
- Cowell, M.R., 1987. Scientific appendix I: chemical analysis. In: Davies, V. (Ed.), Cata-logue of Egyptian Antiquities in the British Museum VII: Axes. British Museum Press, London, pp. 96–118.
- Davey, C.J., Santarelli, B., Rehren, Th., 2021. Egyptian Middle Kingdom copper: analysis of a crucible from Buhen in the Petrie museum. *J. Archaeol. Sci. Rep.* 36.
- Dunham, D., 1943. Notes on copper-bronze in the Middle Kingdom. *J. Egypt Archaeol.* 29, pp. 60–62.
- Dussubieux, L., Deraisme, A., Frot, G., Stevenson, C., Creech, A., Biennu, Y., 2008. LA-ICP-MS, SEM-EDS and EPMA analysis of eastern North American copper-based artefacts: impacts of corrosion and heterogeneity on the reliability of the LA-ICP-MS compositional results. *Archaeometry* 50, pp. 643–657.
- Edwards, D.N., 2004. The Nubian Past. An Archaeology of the Sudan. Routledge, London and New York.
- El Gayar, E.-S., Jones, M.P., 1989a. A possible source of copper ore fragments found at the Old Kingdom town of Buhen. *J. Egypt Archaeol.* 75, pp. 31–40.
- El Gayar, E.-S., Jones, M.P., 1989b. Old Kingdom copper smelting artifacts from Buhen in Upper Egypt. *Histor. Metallurgy* 23, pp. 16–24.
- Farquhar, R.M. and Vitali, V. (2009), Lead isotope analyses of Punic and Roman Artifacts, Unpublished Report, Geophysics Laboratory, University of Toronto, 3p.
- Fleming, S.J., 1982. Lead isotope analyses of Late Period Egyptian bronzes. *MASCA J.* 2, pp. 65–69.
- Gale, N.H., Stos-Gale, Z.A., Maliotis, G., Annetts, N., 1997. Lead isotope data from the Iso-trope laboratory, Oxford: archaeometry data base 4, ores from Cyprus. *Archaeometry* 39, pp. 237–246.
- Gener, M., Montero-Ruiz, I., Murillo-Barroso, M., Manzano, E., Vallejo, A., 2014. Lead provenance study in medieval metallic materials from Madinat al-Zahra (Medina Aza-hara, Córdoba). *J. Archaeol. Sci.* 44, pp. 154–163.
- Gomes, S.S., Valério, P., Alves, L.C., Araújo, M.F., Monge Soares, A.M., Correia, V.H., 2016. Tin determination in fistula seals from Conimbriga and Augusta Emerita. *Microchem. J.* 124, pp. 540–546.
- Hassan, F.A., Tassie, G.J., Rehren, T.H., van Wetering, J., 2015. On-going investigations at the Predynastic to early dynastic site of Kafr Hassan Dawood: copper, exchange and tephra. *Archéo Nil* 25, pp. 75–90.
- Hauptmann, A., 2007. The Archaeometallurgy of Copper. Evidence from Faynan. Springer, Jordan.
- Hauptmann, A., Begemann, F., Heitkemper, E., Pernicka, E., Schmitt-Strecker, S., 1992. Early copper produced at Feinan, Wadi Araba, Jordan: the composition of ores and copper. *Archeomaterials* 6, pp. 1–33.
- Herbert, E.W., 1984. Red Gold of Africa: Copper in Precolonial History and Culture. Uni-versity of Wisconsin Press, Madison.
- Hughes, M.J., 1980. The analysis of Roman tin and pewter ingots. In: Oddy, W.A. (Ed.), Aspects of Early Metallurgy. British Museum, London, pp. 41–50.
- Klemm, R., Klemm, D.D., 2013. Gold and Gold Mining in Ancient Egypt and Nubia. Geoar-chaeology of the Ancient Gold Mining Sites in the Egyptian and Sudanese Eastern Deserts. Springer, Berlin.
- Kmošek, J., Odler, M., Fikrlé, M., Kochergina, Y.V., 2018. Invisible connections. Early Dynastic and Old Kingdom Egyptian metalwork in the Egyptian Museum of Leipzig University. *J. Archaeol. Sci.* 96, pp. 191–207.
- Kuleff, I., Djingova, R., Alexandrova, A., Vakova, V., Amov, B., 1995. INAA, AAS, and lead isotope analysis of ancient lead anchors from the Black Sea. *J. Radioanal. Nucl. Chem.* 196, pp. 65–76.
- Kuleff, I., Iliev, I., Pernicka, E., Gergova, D., 2006. Chemical and lead isotope com-positions of lead artefacts from ancient Thracia (Bulgaria). *J. Cult. Herit.* 7, pp. 244–256.
- Liu, S., Rehren, T.H., Pernicka, E., Hausleiter, A., 2015. Copper processing in the oases of northwest Arabia: technology, alloys and provenance. *J. Archaeol. Sci.* 53, pp. 492–503.
- Marchi, S. et al. (in preparation), Le mobilier de la ville de Kerma (Soudan). Aspects de la vie quotidienne dans la capitale nubienne.
- Masson-Berghoff, A., Pernicka, E., Hook, D., Meek, A., 2018. (Re)sources: origins of metals in Late Period Egypt. *J. Archaeol. Sci. Rep.* 21, pp. 318–339.
- Master, S., Woldai, T., Armstrong, R.A., 2016. The Chaîne des Mongos- a newly discovered Precambrian fold belt in Central African Republic and South Sudan. 35th International Geological Congress. AGI, Cape Town, South Africa 4002.
- Matthäus, H., 1985. Sifnos im Altertum. In: Wagner, G.A., Weisgerber, G. (Eds.), Sil-ber, Blei und Gold auf Sifnos. Prähistorische und antike Metallproduktion, Bochum, pp. 17–58.
- Mödlinger, M., Piccardo, P., 2013. Corrosion on prehistoric Cu-Sn-alloys: the influence of artificial environment and storage. *Appl. Phys. A* 113, pp. 1069–1080.
- Moreau, J.F., Hancock, R.G.V., 1999. The effects of corrosion on INAA characterizations of brass kettles of the early European contact period in northeastern North America. *J. Archaeol. Sci.* 20, pp. 119–1125.
- Nordström, H.A., 1972. Neolithic and A-Group Sites. Scandinavian University Books, Up-psala.
- Odler, M., Kmošek, J., 2020. Invisible Connections. An Archaeometallurgical Analysis of the Bronze Age Metalwork from the Egyptian Museum of the University of Leipzig. Archaeopress, Oxford.
- Odler, M., Kmošek, J., Fikrlé, M., Kochergina, Y.V.E., 2021. Arsenical copper tools of Old Kingdom Giza craftsmen: first data. *J. Archaeol. Sci. Rep.* 36.
- Paparazzo, E., 1994. Surface and interface analysis of a Roman lead pipe “fistula”: mi-crochemistry of the soldering at the join, as seen by scanning Auger microscopy and X-ray photoelectron microscopy. *Appl. Surf. Sci.* 74, pp. 61–72.
- Pernicka, E., Begemann, F., Schmitt-Strecker, S., Grimani, A.P., 1990. On the composition and provenance of metal artefacts from Poliochni on Lemnos. *Oxf. J. Archaeol.* 9, pp. 263–298.
- Pernicka, E., Wagner, G.A., 1985. Die metallurgische Bedeutung von Sifnos im Altertum. In: Wagner, G.A., Weisgerber, G. (Eds.), Silber, Blei und Gold auf Sifnos. Prähistorische und antike Metallproduktion, Bochum, pp. 200–211.
- Pfeiffer, K., 2013. Neue Untersuchungen zur Archaometallurgie des Sinai. Die Entwic-klungsgeschichte Der Innovation “ Kupfermetallurgie”. Leidorf, Rahden/Westfalen.
- Rademakers, F.W., Rehren, T.H., Pernicka, E., 2017. Copper for the Pharaoh: identifying multiple metal sources for Ramesses’ workshops from bronze and crucible remains. *J. Archaeol. Sci.* 80, pp. 50–73.
- Rademakers, F.W., Rehren, Th., Pusch, E.B., 2018a. Bronze production in Pi-Ramesse: alloying technology and material use. In: Ben-Yosef, E. (Ed.), Mining For Copper: Essays in Memory of Professor Beno. University of Tel Aviv, Rothenberg, Tel Aviv, pp. 503–525.
- Rademakers, F.W., Verly, G., Delvaux, L., Degryse, P., 2018b. Copper for the afterlife in Predynastic to Old Kingdom Egypt: provenance characterization by chemical and lead isotope analysis (RMAH collection, Belgium). *J. Archaeol. Sci.* 96, pp. 175–190.
- Rademakers, F.W., Verly, G., Delvaux, L., Vanhaecke, F., and Degryse, P. (in preparation), New perspectives on New Kingdom copper alloys from the RMAH collection, Belgium: elemental and lead isotope data.
- Rademakers, F.W., Verly, G., Delvaux, L., Degryse, P., 2021a. Provenance reinterpretation of some early Egyptian copper alloy artefacts. *J. Archaeol. Sci. Rep.* 38, 103095.
- Rademakers, F.W., Verly, G., Delvaux, L., Vanhaecke, F., Degryse, P., 2021b. From desert ores to Middle Kingdom copper. Chemical and lead isotope data from the RMAH collection, Belgium. *Archaeol. Anthropol. Sci.* 13, p. 100.
- Rademakers, F.W., Verly, G., Marchi, S., Bonnet, C., 2019. A unique casting tech-nology at ancient Kerma: reconstructing furnace technology through experiment, (re-)excavation and archaeometry. Paper presented at the ICA II International Con-ference on Archaeometallurgy 25-29 September 2019.
- Rademakers, F.W., Verly, G., Somaglino, C., Degryse, P., 2020. Geochemical changes dur-ing Egyptian copper smelting? An experimental approach to the Ayn Soukhna process and broader implications for archaeometallurgy. *J. Archaeol. Sci.* 122.
- Rehren, Th., Pernicka, E., 2014. First data on the nature and origin of the metalwork from Tell el-Farkha. In: Mączyńska, A. (Ed.), The Nile Delta As a Centre of Cultural Interactions Between Upper Egypt and the Southern Levant in the 4th Millennium BC, pp. 237–252 Poznan.
- Reisner, G.A., 1923. Excavations At Kerma. Parts IV-V, Harvard African Studies VI. Peabody Museum of Harvard University, Cambridge, MA.
- Renzi, M., Intilia, A., Hausleiter, A., Rehren, Th., 2016. Early Iron Age metal circulation in the Arabian Peninsula: the oasis of Tayma as part of a dynamic network (poster). Proceedings of the Seminar for Arabian Studies 46, pp. 237–246.
- Robbiola, L., Blengino, J.-M., Fiaud, C., 1998. Morphology and mechanisms of formation of natural patinas on archaeological Cu-Sn alloys. *Corros. Sci.* 40, pp. 2083–2111.
- Schwab, R., Willer, F., 2016. Die Zusammensetzung und mögliche Herkunft der Gus-slegierungen. In: Fitzenreiter, M., Willer, F., Auenmüller, J. (Eds.), Materialien Einer Gusswerkstatt von Der Qubbet el-Hawa. EB Verlag, Berlin, pp. 71–81.
- Shortland, A.J., 2006. Application of lead isotope analysis to a wide range of Late Bronze Age Egyptian materials. *Archaeometry* 48, pp. 657–669.
- Spedding, J.V., 2022. Lead isotope analysis of Meroitic period glass from Nubia with LA-MC-ICP-MS. *Archaeometry* doi:10.1111/arc.12780.
- Stos-Gale, Z.A., Gale, N.H., 2010. Bronze age metal artefacts found on Cyprus - metal from Anatolia and the western Mediterranean. *Trab. Prehist.* 67, pp. 389–403.
- Stos-Gale, Z.A., Gale, N.H., Houghton, J., 1995. The origins of Egyptian copper: lead-iso-tope analysis of metals from el-Amarna. In: Davies, V.W., Schofield, L. (Eds.), Egypt, the Aegean and the Levant: Interconnections in the Second Millennium BC. British Museum Press, London, pp. 127–135.
- Stos-Gale, Z.A., Maliotis, G., Gale, N.H., Annetts, N., 1997. Lead isotope characteristics of the Cyprus copper ore deposits applied to provenance studies of copper oxhide ingots. *Archaeometry* 39, pp. 83–123.
- Török, L., 2009. Between Two Worlds. The Frontier Region between Ancient Nubia and Egypt 3700 BC – AD 500. Brill, Leiden.
- Trincherini, P.R., Domergue, C., Manteca, L., Nesta, A., Quarati, P., 2009. The identifica-tion of lead ingots from the Roman mines of Cartagena (Murcia, Spain): the role of lead isotope analysis. *J. Rom. Archaeol.* 22, pp. 123–145.
- Vercoutter, J., Thomas-Goorieckx, D., Lefève, G., 1960. A dagger from Kerma; examina-tion and treatment of a bronze dagger. *Kush* 8, pp. 265–267.
- Verly, G., Rademakers, F.W., Marchi, S., and Bonnet, C. (in preparation), The bronze fur-nace of Kerma revisited. Re-excavation and analysis.
- Walsh, C., 2020. Techniques for Egyptian eyes: diplomacy and the transmission of cos-metic practices between Egypt and Kerma. *J. Egypt. History* 13, pp. 295–332.
- Walsh, C., 2021. Skeuomorphism in Kerma metal vessels. *Sudan and Nubia* 25, pp. 243–251.
- Weeks, L., 2003. Early Metallurgy of the Persian Gulf. Brill Academic Publishers, Inc, Boston/Leiden.
- Weeks, L., Keall, E., Pashley, V., Evans, J., Stock, S., 2009. Lead isotope analyses of Bronze Age copper-base artefacts from al-Midamman, Yemen: towards the identification of an indigenous metal production and exchange system in the southern Red Sea region. *Archaeometry* 51, pp. 576–597.
- Yahalom-Mack, N., Galili, E., Segal, I., Eliyahu-Behar, A., Boaretto, E., Shilstein, S., Finkel-stein, I., 2014. New insights into Levantine copper trade: analysis of ingots from the Bronze and Iron Ages in Israel. *J. Archaeol. Sci.* 45, pp. 159–177.
- Young, S.M.M., 1996. Archaeometric analysis of copper swords from Kerma (Nubia). In: Krzyżaniak, L., Kroeper, K., Kobusiewicz, M. (Eds.), Interregional Contacts in the Later Prehistory of Northeastern Africa. Poznań Archaeological Museum, Poznań, pp. 475–490.